MECHANISM OF ACTION OF CALOXIN

MECHANISM OF ACTION OF CALOXIN

by

MELANIE E.M. HOLMES

A Thesis

Submitted to the School of Graduate Studies

in Partial Fulfillment of the Requirements

for the Degree

Master of Science

McMaster University

August 2002

Master of Science
(Biology)

McMaster University
Hamilton, Ontario

TITLE: Mechanism of Action of Caloxin

AUTHOR: Melanie E.M. Holmes, B.Sc. (McMaster University)

SUPERVISOR: Dr. A.K. Grover

OF PAGES: xi, 84

ABSTRACT

The plasma membrane Ca^{2+}-pump (PMCA) is a Ca^{2+}-Mg^{2+}- ATPase that expels Ca^{2+} from cells to help them maintain low concentrations of cytosolic Ca^{2+}. Four genes (PMCA1 to PMCA4) encode various isoforms of this pump. Caloxin is a novel peptide that was selected for binding to the second putative extracellular domain of PMCA1. Caloxin inhibits the Ca^{2+}- Mg^{2+}-ATPase in human erythrocyte leaky ghosts which primarily contain PMCA4. The objectives of this thesis are to delineate the mechanism of this inhibition and to determine its PMCA isoform selectivity.

Caloxin inhibition of the PMCA pump in erythrocyte ghosts is non-competitive with respect to the substrates Ca^{2+} and ATP and the activator calmodulin. This was expected because the high affinity binding site for Ca^{2+} and sites for ATP and calmodulin are intracellular whereas caloxin is a peptide selected for binding to the second extracellular domain of the pump. In the reaction cycle, PMCA forms a 140 kDa acylphosphate enzyme intermediate from ATP (forward reaction) or orthophosphate (reverse reaction). Caloxin inhibits the acylphosphate formation in the forward but not in the reverse reaction. These results suggest that caloxin inhibits conformational changes required during the reaction cycle of the pump.

In COS-M6 cells overexpressing PMCA4, caloxin inhibited the Ca^{2+}-Mg^{2+}-ATPase but with a marginally lower affinity than in the erythrocyte ghosts. Caloxin inhibition was also observed in insect cells overexpressing PMCA2. Several unsuccessful attempts were made to overexpress functional PMCA1. The work on

isoform selectivity would require high level of expression of various PMCA isoforms and problems related to this requirement are discussed.

Caloxin appears to inhibit the PMCA pumps by binding to the second putative extracellular domain and thus affecting the conformation of the protein. This is the first identified role of an extracellular domain of a PMCA pump.

ACKNOWLEDGEMENTS

I would like to express my sincere appreciation to my supervisor, Dr. Grover, for teaching, supporting and challenging me during my graduate training. I am inspired by his dedication to his students, to research and to the game of golf. I would also like to thank the other members of my supervisory committee, Dr. Daniel and Dr. Werstiuk, for their helpful comments and encouragement.

I am fortunate to have had the opportunity to work with an amazing group of individuals during my studies. This thesis would not have been possible without their support, guidance and friendship. I am deeply indebted to Christine Misquitta for her continuous support, as both mentor and friend. I truly believe that I would not be where I am today without her help. She introduced me to the field of research during my undergrad and she has been a constant source of advice and encouragement ever since.

I would also like to thank Sue Samson for the guidance and technical expertise that she provided and Christina Beaver for her careful efforts and helpful comments proofreading this document.

I thank James Mwanjewe for taking a genuine interest in my ideas and for always making himself available to help me, even at a moment's notice. I am also thankful for the support provided by Lin Nie - her smile could always brighten my day, especially when things weren't going right.

I express my gratitude and deep appreciation to Mandy Walia and Jyoti Pande whose friendship, knowledge and wisdom have supported, enlighted and entertained me over the years of our friendship. Thank you both for always listening and for making me

feel as though everything would be o.k, especially when things got tough. I will miss our coffee breaks between experiments, our conversations about life and the laughter that we shared.

My deepest gratitude goes to my family, especially Mom and Dad for their unconditional support and love and to Sarena, Jennifer, and Patrick for taking much needed coffee breaks with me. Finally, I would like to thank Christopher Tan for his friendship, love and support and more importantly, for helping me see the light at the end of the tunnel.

TABLE OF CONTENTS

LIST OF ILLUSTRATIONS

Figure number

LIST OF ABBREVIATIONS

AMP-PCP	beta,gamma-methylene-adenosine-5'-triphosphate
BSA	bovine serum albumin
$[Ca^{2+}]_i$	cytosolic Ca^{2+} concentration
Caloxin 2A1	caloxin
DAG	1,2-diacylglycerol
DMEM	dulbecco's modified eagles's medium
DMSO	dimethylsulfoxide
Dox	doxycycline
DTT	1-4-dithiothreitol
EC	extracellular
EDTA	(ethylenedinitrilo)-tetraacetic acid ethylene glycol
EGFP	enhanced green fluorescence protein
EGTA	ethylene glycol-bis(ß-aminoethyl ether)-N, N, N', N'-tetraacetic acid
ER/SR	endoplamic/sarcoplasmic reticulum
HEPES	4-(2-hydroxyethyl-1-piperazine ethane sulfonate)
IC	intracellular
IP_3	inositol 1,4,5-trisphosphate
Ki	inhibition constant
MES	2-[N-Morpholino]ethanesulfonic acid
MOPS	3[N-morpholino]propane sulfonate-NaOH
OPA	one-phor-all buffer
PBS	phosphate buffered saline
PED	putative extracellular domain
PEP	phospho(enol)pyruvate
Pi	inorganic phosphate
PIP_2	phosphatidylinositol 4,5-bisphosphate
PKA	protein kinase A
PKC	protein kinase C
PM	plasma membrane
PMCA	plasma membrane calcium ATPase
PMSF	phenylmethylsulfonyl fluoride
RACC	receptor-activated calcium channels
RYR	ryanodine sensitive Ca^{2+}-release channels
SEM	standard error of the mean
SERCA	sarco/endoplasmic reticulum calcium ATPase
SOCC	store-operated calcium channels
TM	transmembrane
TNP-ADP	2'(3')-O-(2,4,6-trinitrophenyl)adenosine 5'-diphosphate
Tris	tris (hydroxymethyl) aminomethane
VOCC	voltage-operated calcium channels

1.0 INTRODUCTION

1.1 Calcium Homeostasis

1.1.1 *Overview*

Calcium (Ca^{2+}) is an important signaling ion, controlling a wide variety of cellular processes, including the synthesis and release of hormones, muscle and non-muscle motility and nervous activity (2, 12). Changes in the cytosolic free calcium ion concentration $[Ca^{2+}]_i$ constitute one of the main pathways by which information from extracellular signals is transferred to intracellular sites (2, 7). In the resting cell, the $[Ca^{2+}]_i$ is less than 0.1 μM, 10,000-fold lower than the external $[Ca^{2+}]$ (30). Very high concentrations of Ca^{2+} are also present in intracellular organelles such as the endoplasmic/sarcoplasmic reticulum (ER/SR). Thus there is a large electrochemical gradient across the plasma membrane (PM) and ER/SR membrane that favors Ca^{2+} movement into the cytosol (64). This gradient is important for cell survival and signaling and is maintained by a variety of proteins, which are either soluble or intrinsic to membranes (12, 56). Upon activation of a cell, calcium rushes into the cytosol through various Ca^{2+} channels in either of these membranes, triggering Ca^{2+}-responsive proteins in the cell. Following the signaling event, the $[Ca^{2+}]_i$ must return to low resting levels. This is achieved by Ca^{2+} pumps in the PM and ER/SR, and/or the Na^+-Ca^{2+} exchanger in the PM (52, 56).

1.1.2 *Mechanisms to Increase $[Ca^{2+}]_i$*

1.1.2.1 *Ca^{2+} entry from the extracellular space*

There are two main pathways by which extracellular Ca^{2+} can enter cells. These include voltage-operated Ca^{2+} channels (VOCCs) and receptor-activated Ca^{2+} channels (RACCs). VOCCs are controlled by depolarization of the plasma membrane (52). Traditionally VOCCs have been associated with excitable cells, however they are also present in a number of non-excitable cell types including glial cells, myeloma cells and osteoblasts (52). There are several subtypes of VOCCs, including L-, T-, N- and P-type channels, with L-type channels appearing to be the most widely distributed. Electrical and pharmacological properties, as well as tissue specificity distinguish the channel subtypes (12, 52).

RACCs open as a result of the binding of an agonist to its receptor, a protein that is separate from the channel protein. The receptor is linked to the Ca^{2+} channel by a mobile intracellular messenger such as a trimeric G-protein (7). Of all the PM Ca^{2+} channels, the RACCs are the most poorly understood, due in part to the large number of RACC subtypes (differentiated mainly on the basis of ion selectivity and mechanism of channel opening) (7, 21). One major subfamily of RACCs is the store-operated Ca^{2+} channels (SOCCs) (21, 39). These channels open in response to a decrease in Ca^{2+} concentration in the ER/SR. The mechanism(s) by which SOCCs are activated are not well understood, however current hypotheses include the conformational coupling (protein-protein interaction between SOCC protein and IP_3 sensitive Ca^{2+} channel protein in the ER/SR) and the mobile intracellular messenger (Ca^{2+} influx factor release from the ER/SR) hypotheses (21, 39, 52).

1.1.2.2 *Ca^{2+} release from intracellular stores*

The ER/SR is the main intracellular Ca^{2+} store from which Ca^{2+} can be released in response to different stimuli, thereby increasing the $[Ca^{2+}]_i$. There are two kinds of Ca^{2+} channels present in the ER/SR, which are different from those observed on the plasma membrane and are independent of voltage: inositol 1,4,5-trisphosphate (IP_3) -sensitive Ca^{2+} channels and ryanodine sensitive Ca^{2+}-release channels (52). In the IP_3 signaling pathway, an agonist (for example, noradrenaline, acetylcholine or serotonin) interacts with its receptor on the plasma membrane leading to a signaling cascade that results in the hydrolysis of phosphatidylinositol 4,5-bisphosphate (PIP_2) to IP_3 and 1,2-diacylglycerol (DAG) (2, 8). IP_3 is an intracellular messenger that binds to IP_3-sensitive Ca^{2+} channels on the ER/SR, mobilizing Ca^{2+} from this organelle (2, 77). Opening of IP_3-sensitive Ca^{2+} channels is potentiated by cytosolic Ca^{2+} ions, which increases the affinity of the receptor for IP_3, resulting in greater release of stored Ca^{2+} (2, 8). High concentrations of cytosolic Ca^{2+} however, inhibit IP_3 induced Ca^{2+} release by decreasing the affinity of the receptor for IP_3 (2, 8).

In addition to IP_3-sensitive Ca^{2+} channels, muscle cells and neurons possess ryanodine sensitive Ca^{2+}-release channels (RYRs) (2, 52). These channels are structurally similar to the IP_3 sensitive Ca^{2+} channels and were named for their sensitivity to the plant alkaloid ryanodine (2, 52). In skeletal muscle cells, RYRs located in the SR membrane associate with voltage-sensitive proteins in the plasma membrane. When voltage-sensitive proteins are activated by an action potential, they trigger some of the RYRs to open (2, 52). The Ca^{2+} ions that are released through these channels stimulate

more RYRs to open, thereby amplifying the response (12, 52). However unlike IP_3-sensitive Ca^{2+} channels, RYRs are not inhibited by high $[Ca^{2+}]$ (2, 12, 52).

1.1.3 *Mechanisms to reduce $[Ca^{2+}]_i$*

The signaling function and the survival of cells requires that the $[Ca^{2+}]_i$ be maintained at low levels (2, 56). Systems such as the *Na^+-Ca^{2+} exchanger*, and active transport of Ca^{2+} by *Ca^{2+} pumps* are important mechanisms for reducing $[Ca^{2+}]_i$ (9, 28, 56). Mitochondria are capable of accumulating Ca^{2+} via a uniporter driven by the electrochemical proton gradient across the inner mitochondrial membrane. However its involvement in Ca^{2+} homeostasis is generally believed to occur only when the $[Ca^{2+}]_i$ rises to toxic levels (56). The contribution of these systems to the maintenance of calcium homeostasis varies from one cell type to another and depends on several factors (see section 1.4).

The *Na^+-Ca^{2+} exchanger* is a low-affinity, high-capacity carrier of Ca^{2+}. Its contribution to Ca^{2+} homeostasis varies from tissue to tissue, with it being most active in heart and neuronal cells (9, 71). Its activity is driven by the transmembrane Na^+ gradient and is sustained by the Na^+-K^+-ATPase. Typically, the system transports one Ca^{2+} ion out of the cell in exchange for three Na^+ ions, thus operating electrogenically (9, 71). The exchanger can also contribute to Ca^{2+} entry into the cell, depending on the electrochemical gradients of Na^+ and Ca^{2+} and the membrane potential of the cell (9, 56, 71). However, the Ca^{2+} affinity of the exchanger is too low to account for the submicromolar levels of Ca^{2+} in the resting cell. Therefore, the essential task of

continuously regulating Ca^{2+} below the micromolar range very likely demands the function of Ca^{2+} pumps (15).

There are two types of *Ca^{2+} pumps,* which use the energy of hydrolysis of ATP to move calcium against its concentration gradient (28). Compared to the Na^{+}-Ca^{2+} exchanger, the Ca^{2+} pumps have high affinity, but low capacity to transport Ca^{2+} (28). The plasma membrane Ca^{2+} pump (PMCA) expels Ca^{2+} from the cytosol to the extracellular space. The sarcoplasmic/endoplasmic reticulum Ca^{2+} pump (SERCA) sequesters cytosolic Ca^{2+} into this organelle (28). Both pumps consist of a single polypeptide; PMCA is 140 kDa and SERCA is 110 kDa. Furthermore, PMCA and SERCA pumps share both structural (32% identity at the primary sequence level) and mechanistic properties (13, 28). Both pumps form a transient phosphorylated enzyme intermediate from ATP (involving a conserved aspartic acid residue), which is necessary for translocation of Ca^{2+} (57) (see section 1.2.1). For every ATP hydrolyzed, the skeletal muscle SERCA1 pump transports 2 Ca^{2+} ions (49). The stoichiometry of ATP hydrolyzed to Ca^{2+} ions transported is not well established for the PMCA pump; however, the observation that the Hill coefficient for activation of the ATPase by Ca^{2+} in erythrocytes approaches 1, suggests a 1:1 stoichiometry for PMCA (13).

Despite the similar function of PMCA and SERCA pumps, they have different regulatory properties. Regulation of pump activity by phospholamban is a distinct property of the SERCA pump, whereas calmodulin appears to regulate the activity of both pumps (31, 43). Modulation of the PMCA pump, however, is not limited to its activation by calmodulin. There exist a number of other mechanisms designed to alter PMCA pump activity, which will be discussed in greater detail in section 1.2.3.

1.2 PMCA

1.2.1 *Discovery of PMCA and its mechanism of ion translocation*

The existence of a Ca^{2+}-ATPase was first reported in the erythrocyte membrane by Dunham and Glynn (1961) (13). Schatzmann (1966) connected it to the pumping of Ca^{2+} out of the cell by demonstrating that Ca^{2+} emerged from Ca^{2+}- and ATP-loaded sealed ghosts at a higher rate than from cells treated without the addition of ATP, even in media containing higher Ca^{2+} concentrations than inside the ghosts (70). After this observation, the erythrocyte was the primary experimental subject used to study the properties of the pump (13). Only much later was the work extended to other cells, showing that ATP-dependent pumping of Ca^{2+} is a general property of the plasma membranes of all cells, including those from "excitable" cells where it was generally assumed that the Na^{+}-Ca^{2+} exchanger was the only Ca^{2+} exporting system (9, 13).

Partial sequencing work revealed that the PMCA pump shared regions of homology with ATPases belonging to the family of P-type ion-motive pumps (57). Members of this family (which includes SERCA and the Na^{+}-K^{+}-ATPase) mediate active ion transport coupled to ATP hydrolysis through formation and breakdown of a phosphorylated enzyme intermediate (an aspartyl-phosphate) (54, 57). Formation of the phosphorylated intermediate occurs on a conserved aspartic acid residue in the catalytic domain of these pumps (54, 57). The region where ATP binds these pumps is also conserved as assessed by fluorescein isothiocyanate (FITC)-binding (23).

The mechanism of active Ca^{2+} transport by PMCA follows the same general model of all other P-type ion pumps (49, 57). The model proposes that the pump alternates between two distinct conformational states, E1 and E2 (3, 49, 57). These two

states differ in that the pump's affinity for Ca^{2+} is high in the E1 conformation and low in the E2 conformation (3, 17, 57). These conformations also differ in their affinities for Mg^{2+}, ATP and ADP. Fig. 1 outlines the partial reactions of the catalytic and transport cycle of PMCA. It begins with the binding of Ca^{2+} to the high affinity Ca^{2+}-binding sites (Km 0.2-7 μM) of the E1 form of the enzyme (3, 13, 49). Ca^{2+} binding is followed by the binding of ATP to its high affinity binding site (Km 1-2.5 μM) (3, 13, 49). An aspartic acid residue in the active site (Asp 475 in human PMCA1b isoform) is then phosphorylated, resulting in a conformational change of the $E1PCa^{2+}$ phosphoenzyme intermediate to the $E2PCa^{2+}$ form, which has decreased Ca^{2+} affinity (14). Following release of Ca^{2+} to the extracellular space, Mg^{2+}-catalyzed hydrolysis of E2P results in the release of inorganic phosphate (Pi), leaving E2 (13). The hydrolysis of E2P is assumed to be accelerated by the binding of ATP to a site on the pump that has less affinity (Km 145-180 μM) than the site that binds ATP to initiate phosphorylation (13, 68). In the final step of the reaction cycle, the enzyme returns to the E1 conformation and often involves the counter transfer of other cations (2 K^+ for Na^+-K^+-ATPase and 1 or 2 H^+ for PMCA) (13, 34, 63).

It is important to note that in Fig. 1, the phosphorylation reactions are reversible (3, 17, 57). The phosphorylated pump can react with ADP in the presence of Ca^{2+} to regenerate ATP (3, 57). The dephosphorylation event is also reversible, so that incubation of the pump with Pi in the absence of Ca^{2+} leads to formation of an acid-stable phosphorylated intermediate that is presumed to be the E2 form of the enzyme (3, 17).

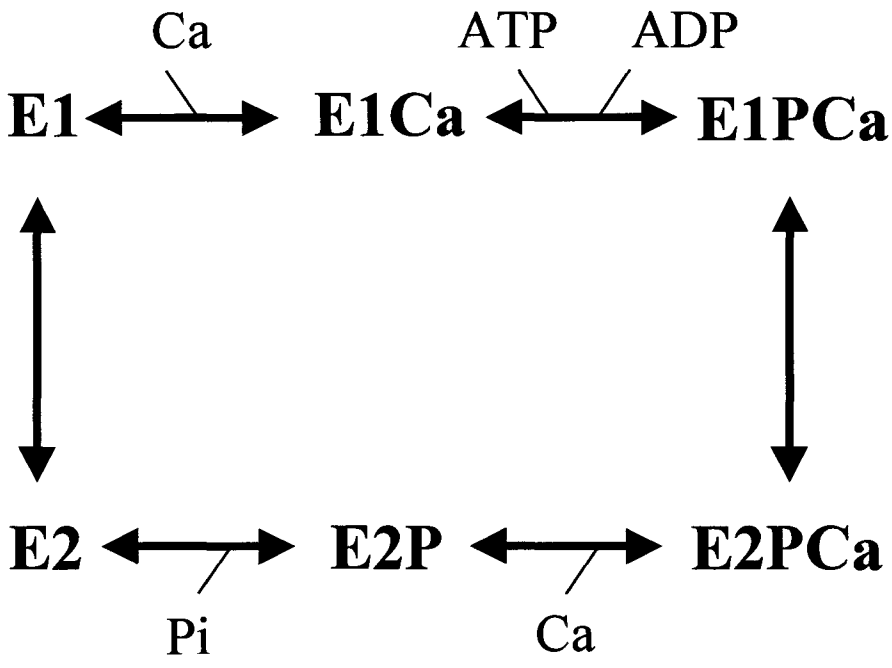

Fig. 1: E1-E2 reaction scheme for the Ca^{2+}-Mg^{2+} ATPase. The scheme is based on the assumption of two major conformational states, E1 and E2, which are characterized by their ability to become phosphorylated by ATP and Pi respectively (57).

1.2.2 *Structural Characteristics of PMCA*

The primary structure of PMCA was deduced in 1988 by Shull and Greeb from cDNA isolated from rat brain, by Verma et al. from a human teratoma cell cDNA library, and in 1991 by Khan and Grover from smooth muscle cDNA library (46, 72, 82). Based on hydrophobicity analysis of the PMCA pump's primary structure, combined with secondary structure predictions, antibody binding studies and information on the domain organization of fast skeletal muscle SERCA1, a structural model for the PMCA pump has been formulated (12, 22, 38, 72, 82). This model proposes a protein with 10 putative *transmembrane* (TM) spanning domains, which are connected in the *extracellular* (EC) space by 5 short peptide chains (EC domains) (13). The cytosolic location of the NH2- and COOH termini suggest an even number of TM domains however the exact number (8 vs. 10) is still tentative. A monoclonal antibody has been found to recognize an external epitope in the EC domain connecting the first and second TM domains (22). Therefore, only the topology of the first EC domain has been verified. Extracellular domains 2-5 are still putative. Further discussion will utilize the 10 TM domain model. The TM domains may play a role in high affinity Ca^{2+}-binding and translocation across the membrane, as mutagenesis of specific residues within TM domains 4, 6 and 8 of PMCA (and TM domains 4, 5, 6 and 8 of SERCA) cause loss of Ca^{2+} transport and Ca^{2+}-dependent formation of the phosphorylated enzyme intermediate (17, 33).

The bulk of PMCA's mass protrudes into the cytosol with most of the known properties of the pump having been assigned to its 3 most prominent *intracellular* (IC) domains (13-15). The first IC domain, a loop between putative TM domains 2 and 3, corresponds to the transduction domain of other P-type ion pumps, and may be involved

in coupling ATP hydrolysis to Ca^{2+} translocation (49, 57). It also contains a region that is responsive to acidic phospholipids (see section 1.2.3.2) (13, 83). The second, and largest IC domain (430 residues) connects TM domains 4 and 5, and is termed the catalytic domain. This domain contains the catalytic sites of the pump, including the conserved aspartic acid residue that forms the high-energy phosphorylated intermediate during ATP hydrolysis and, about 140 residues downstream, the site of ATP binding (15, 23). A hinge region formed by two alpha-helices, is postulated to have sufficient flexibility to allow these two catalytic sites to come together during the reaction cycle (13-15). The third IC domain, termed the regulatory domain, is the COOH-terminal tail that protrudes from 10^{th} TM domain. This domain is longer in PMCA than in SERCA and contains the major regulatory sites of the pump, including the calmodulin binding domain and another site for regulation by acidic phospholipids (15, 28, 43). The calmodulin binding domain is flanked by acidic residues which have been proposed to be sites for low affinity Ca^{2+} binding. These Ca^{2+} binding sites are different from the high affinity Ca^{2+} binding sites involved in the catalytic cycle, since proteolytic treatments that remove them together with the calmodulin-binding domain leave a truncated enzyme that still possesses high Ca^{2+} affinity (13-15). The regulatory mechanisms of the pump will be discussed in greater detail in the section to follow.

1.2.3 *Regulatory mechanisms of PMCA*

1.2.3.1 *Calmodulin stimulation*

Hemolysate was found to contain a modulator protein that increased the Ca^{2+}-stimulated ATPase activity of erythrocyte ghosts beyond the level achieved with addition

of Ca^{2+} alone (42). This protein was purified from erythrocytes and was subsequently identified as calmodulin (43). Direct binding of Ca^{2+}-calmodulin to PMCA increases the pump's affinity for Ca^{2+} and its maximal transport rate (44). With the use of calmodulin-depleted erythrocyte membranes, the Km (Ca^{2+}) of the pump has been found to decrease from 30 μM to below 1 μM while the maximal rate of transport may increase up to 10 times (13, 44, 58). These effects can be explained in terms of an increase in the turnover of the PMCA pump by Ca^{2+}-calmodulin. Accordingly, Ca^{2+}-calmodulin has been found to increase both the rate of PMCA's ATP-promoted phosphorylation and that of its dephosphorylation (44, 58).

Controlled proteolysis of the purified erythrocyte Ca^{2+} pump using trypsin, has helped elucidate the location of the calmodulin binding domain within the pump molecule (13). Trypsin mimicked the effects of Ca^{2+}-calmodulin and showed that the activated pump was no longer stimulated by calmodulin. Trypsin removed from the cytosolic side of the enzyme, a 30 kDa fragment, which was suggested to contain the calmodulin binding domain of the pump (13). The primary sequence of the calmodulin binding domain was eventually determined using erythrocytes, and was localized to a region in the COOH-terminus, approximately 40 residues downstream of the last TM domain (41). In the absence of Ca^{2+}-calmodulin, this sequence acts as an autoinhibitory domain, preventing catalytic turnover (13, 20). Cross-linking studies using labeled peptides demonstrated that the calmodulin binding domain interacts with two intramolecular regions of the pump, one located in the first cytosolic loop and the other in the catalytic domain between the phosphorylation and the ATP binding site (13, 20). In the absence of Ca^{2+}-calmodulin, the autoinhibitory domain is thought to prevent catalytic

turnover by occluding the catalytic sites from their substrates. An increase in Ca^{2+}-calmodulin following a rise in intracellular Ca^{2+} levels causes Ca^{2+}-calmodulin to bind to the autoinhibitory domain of PMCA, thereby releasing the inhibition and stimulating the pump (13-15).

1.2.3.2 *Acidic phospholipids*

Experiments using purified PMCA from erythrocytes have supported the ability of acidic phospholipids to activate the pump (61, 62). Niggli et al (1981) showed that acidic phospholipids (phosphatidlyserine, phosphatidylinositol and phosphatidic acid) increased the Vmax and decreased the Km (Ca^{2+}) whereas neutral phospholipids (phosphatidylcholine, sphingomyelin and phosphatidylethanolamine) had no effect (62). In fact, acidic phospholipids, phosphatidylinositol in particular, activate the pump to a higher extent than calmodulin (they reduce the Km (Ca^{2+}) below that achieved with calmodulin) (13). Activation by acidic phospholipids renders PMCA insensitive to calmodulin activation however acidic phospholipids can further reduce the Km (Ca^{2+}) of the calmodulin stimulated pump, suggesting separate binding sites for phospholipids and calmodulin (13). This idea was supported by proteolysis work which showed that sequential removal of portions of the pump led first to the loss of calmodulin stimulation and then to the loss of the stimulatory effects of acidic phospholipids (13). The phospholipid effect could be important in vivo since the PMCA is embedded in an environment containing high concentrations of acidic phospholipids, suggesting that it would be in a partially active state permanently (61).

1.2.3.3 *Phosphorylation by protein kinases*

Phosphorylation by two protein kinases (PK), PKA and PKC, also modulates the activity of the PMCA. The cAMP-dependent PKA increases both the Vmax and the affinity of the pump for calcium (13-15). Phosphorylation by PKC is more complex. Earlier reports describe a large increase in the Vmax without changes in Km (Ca^{2+}) however later studies suggest activation by PKC is smaller and competitive to the activation by calmodulin (13-15). Studies have suggested that the phosphorylation sites for both PKA and PKC reside in the COOH terminus, which is rich in serine and threonine residues. The phosphorylation seems to be isoform specific and affects the PMCAs in very different ways (19).

1.2.3.4 *Activation through proteolysis*

Proteolysis experiments using trypsin were important in the identification of the functional domains of the pump (13-15). The effects of the intracellular protease calpain, are likely to be significant in vivo, since calpain is preferentially targeted to proteins containing calmodulin binding domains (14). Calpain has been shown to activate PMCA in its native membrane environment and in a purified state, though much more slowly than trypsin. Calpain truncates the pump COOH terminally removing in two steps, the calmodulin binding domain, leaving a fully active 124 kDa fragment (13-15). This fragment persists for some time however it is eventually degraded, possibly by other proteases. The concentration of Ca^{2+} required to activate calpain exceeds 1 μM, questioning the physiological significance of calpain degradation in a healthy cell (13-15).

1.3 *Isoforms of PMCA & their tissue-specific patterns of expression*

PMCA belongs to a multigene family composed of at least four members, PMCA1, PMCA2, PMCA3 and PMCA4 (15). These isoforms were discovered by screening mammalian cDNA libraries with the majority of work performed on human and rat (27, 72, 75). The positions of the four human genes have been mapped to the following chromosomes: isoform 1 maps to chromosome 12 (q21-q32), isoform 2 to chromosome 3 (p25-p26), isoform 3 to the X chromosome (q28) and isoform 4 to chromosome 1 (q25-q32) (76). Each of these genes produces additional isoform variability by alternative splicing of their primary transcripts. Over 20 splice variants have been detected at the RNA level (76). Splicing can occur at two sites, defined as site A and site C. Site A is located immediately upstream of the phospholipid binding region in the first intracellular domain of the pump. Splicing at site C involves the calmodulin binding domain and occurs in all four isoforms (45, 76).

Comparison of the tissue distribution of the mRNA encoding the four pump isoforms suggests that PMCA1 and PMCA4 are most widely expressed (10, 45, 74). These two isoforms are expressed in all tissues examined so far, with isoform 1 being more abundant than isoform 4, the exception being erythrocytes (74, 75). Isoforms 2 and 3 are expressed in a tissue-specific manner, being found mainly in brain and muscle (10, 74). Within the brain, PMCA2 is expressed primarily within Purkinje cells of the cerebellum and in cochlear hair cells (lower levels are also found in the heart, liver, kidney, uterus) (10, 18, 74). For PMCA3, expression is highest in the choroid plexus of the brain (lower levels found in skeletal muscle and testes) (10, 74). The expression

patterns, therefore, suggest that the brain expresses the greatest abundance and diversity of PMCA isoforms and splice variants (24).

1.4 *The Physiological Role of PMCA in Ca^{2+} Homeostasis: Challenges*

The contribution of the PMCA pump to intracellular Ca^{2+} homeostasis cannot be assessed without considering the role of other Ca^{2+} transporting systems that exist within various tissues. Furthermore, a number of factors will influence the Ca^{2+} handling dynamics of each of these systems. Some of these factors include: 1) the demands of the cell for Ca^{2+} (how much Ca^{2+} must be moved at rest, as well as during and following activity), 2) the capabilities of the various Ca^{2+} transporting proteins (affinity for Ca^{2+} and turnover number), 3) the densities of various systems and 4) localization and spatial relationship of various Ca^{2+} transporting proteins within the cell (even dispersal versus localization to caveolae for example) (9).

Due to the high affinity of the PMCA pumps for Ca^{2+}, they have traditionally been assigned the role of maintaining basal levels of intracellular Ca^{2+} (13, 76). In contrast, the Na^+-Ca^{2+} exchanger, with a low affinity but high capacity for Ca^{2+}, is thought to be the primary mechanism for rapidly removing large amounts of intracellular Ca^{2+} when $[Ca^{2+}]_i$ is elevated and the driving force is large (9). The role of the Na^+-Ca^{2+} exchanger as the primary Ca^{2+} extrusion mechanism in the heart is widely accepted, although in other tissues, there is limited evidence suggesting that the PMCA pump may dominate (25). *Muallem et al (1988)* studied the relative contributions of the Na^+-Ca^{2+} exchanger and the PMCA pump on calcium efflux from stimulated rat pancreatic acini cells. Changing the Na^+ gradients across the PM had minimal effects on resting $[Ca^{2+}]_i$,

the rate constant of calcium efflux, and $[Ca^{2+}]_i$ levels attained after 5 min of stimulation, suggesting that calcium efflux is mediated primarily by the PMCA pump (59). Furthermore, mechanoelectrical transduction channels of hair cells of the inner ear are permeable to calcium, which regulates adaptation of hair bundles, the sensory organelle involved in hearing and balance. However, the ionic composition of endolymph is incompatible with Ca^{2+} extrusion via the Na^+-Ca^{2+} exchanger, hence hair cells rely on PMCA, a protein that is highly concentrated in hair bundles (18, 25). *Kozel et al (1998)* studied the phenotype of mice null for any functional PMCA2. These mice had distinct hearing and balance impairments in addition to anatomical deformities of the cerebellum and inner ear (47). Finally, *Husain et al. (1997)* suggested a critical role for PMCA, as opposed to the Na^+-Ca^{2+} exchanger, in the regulation of vascular smooth muscle cell proliferation (40). However, these studies do not take into account a possible coupling due to co-localization of PMCA pumps with activation of individual receptors. Nor do they consider coupling between various other pathways. For example, a close proximity between the Na^+-Ca^{2+} exchanger and SERCA has been reported in some tissues (9, 71). Others have reported that transporters may be co-localized in caveolae which may contribute to unique Ca^{2+} mobilization pathways (84). Another limitation of these studies was the absence of a specific PMCA inhibitor. In fact, ***the lack of a specific pharmacological inhibitor of PMCA has been a major impediment to determining its physiological role in the cell.*** Vanadate, lanthanum and fluorides inhibit PMCA non-selectively and have been valuable as tools for studying the reaction mechanism of PMCA (13, 55, 78). However, these compounds also inhibit other ATPases (such as SERCA and the Na^+-K^+-ATPase) with different affinities. For example, the Na^+-K^+-

ATPase has an extremely high affinity for vanadate whereas PMCA has a low affinity for this compound (11, 78). Therefore these non-specific inhibitors are unsuitable for determining the physiological role of PMCA in an intact cell. Na^+-K^+-ATPase inhibitors, ouabain and digoxin, and SERCA pump inhibitors thapsigargin and cyclopiazonic acid, have played important roles in elucidating how these pumps affect cell function (26, 69, 80). Thus, a selective PMCA pump inhibitor is required to determine the role of this pump in cellular Ca^{2+} homeostasis and signal transduction.

1.5 Caloxin: A Novel and Specific Inhibitor of PMCA

Recently, we reported caloxin 2A1 (16). Caloxin 2A1 was found to inhibit the Ca^{2+} pump activity of the erythrocyte plasma membrane (16). Caloxins have been defined as "substances that bind to one of the 5 putative extracellular domains (PED1 to 5) of the PMCA pump to alter its activity". The sequences of PED 1 to 5 for PMCA isoforms 1 to 4 are given in Fig. 2. All of the known functional properties of the PMCA are assigned to the IC or TM domains of the pump (13-15). The design of caloxins however, was based on the hypothesis that perturbing the extracellular domains would alter the function of the pump. Further rationale for the design of caloxins came from experiments on the Na^+-K^+-ATPase which showed that a monoclonal antibody against an extracellular sequence of the pump inhibited its activity (4). Since both PMCA and the Na^+-K^+-ATPase display structural similarities, perturbation of the extracellular domains of PMCA was expected to affect its activity also.

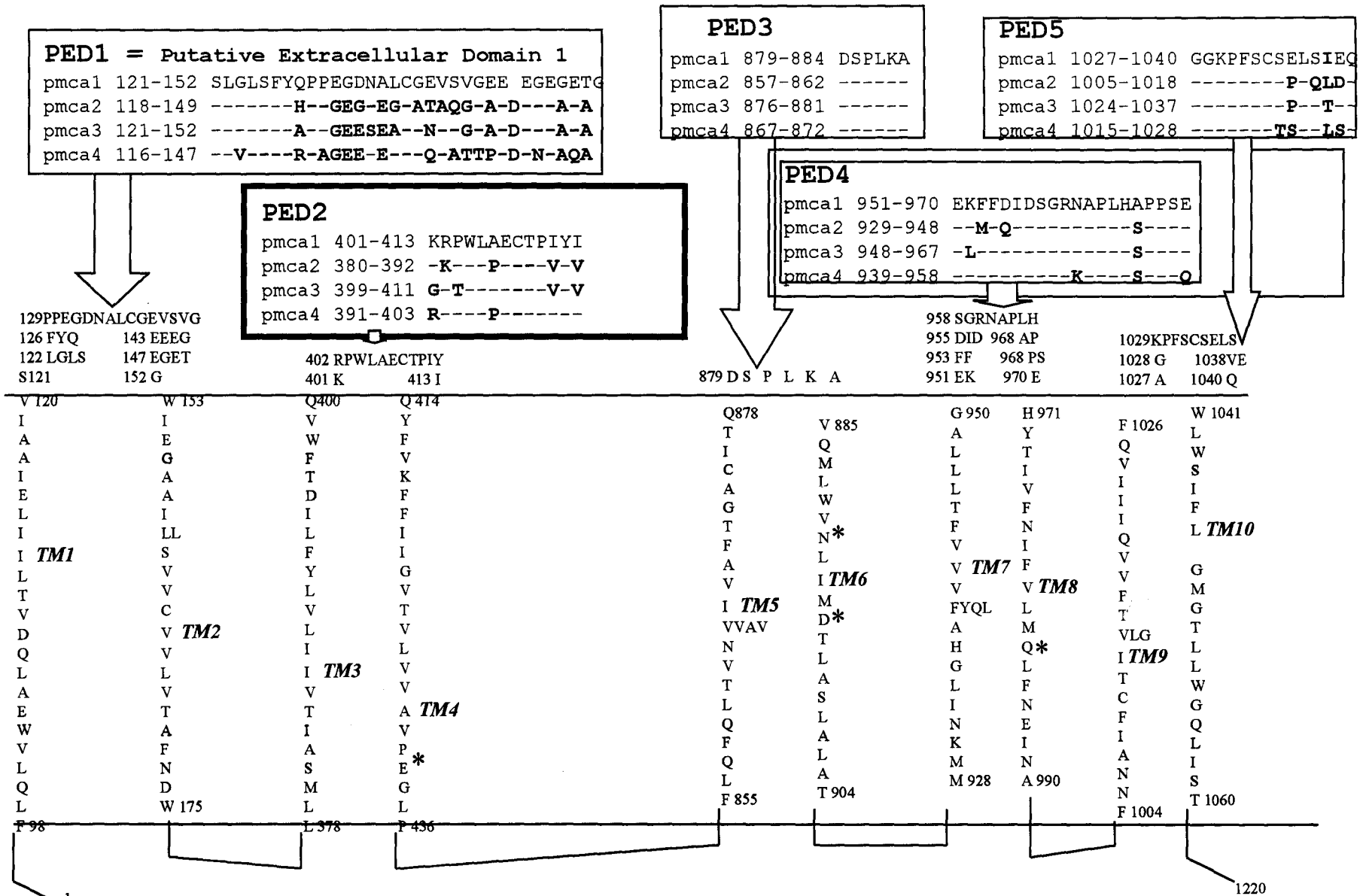

Fig. 2: PMCA1 STRUCTURE. The model is for rabbit PMCA1b (Khan & Grover,Genbank X59069). Comparison of PMCA1 to 4 are for human (Swiss protein bank accession # P20020, Q01814, Q16720, P23634). Identical residues are marked as "-". Transmembrane residues in PMCA4 whose mutation to A cause loss of ATPase activity and acylphosphate formation from ATP: E423, N879, D883, Q971. Corresponding residues in PMCA1 sequence are marked with " * ". Cytoplasmic Sites of Interest: 461-D: Acylphosphate site, 598-IFSKGASEILK: FITC binding site, 1080 - EIGEEELAEDVEEIV: Autoinhibitory site, 1098 - RELRRWQILWFRLNRIQ: calmodulin binding site, 1174 - KRNNS: cAMP-dependent phosphorylation site.

Caloxin 2A1 was designed by screening a random peptide phage display library for binding to the PED2 sequence (residues 401-413, KRPWLAECTPIYI) of PMCA1b. Caloxin 2A1 is a 15 amino acid peptide, composed of the following amino acids - VSNSNWPSFPSSGGG-amide (16). The sequence of PED2 in PMCA1b is similar to the corresponding sequences in PMCA2, 3 and 4 (Fig. 2) however in PMCA4 and PMCA2, an alanine residue is replaced by a proline. In PMCA3, a proline is replaced by a threonine and a lysine is replaced by a glycine residue. It remains to be determined whether or not these amino acid substitutions, which vary in structure, size and electric charge, affect the tertiary structure of PED2 in PMCA2, 3 and 4 and consequently, the binding sites for caloxin 2A1.

In erythrocyte leaky ghosts that contain primarily PMCA4, caloxin 2A1 inhibited the Ca^{2+}-Mg^{2+}-ATPase, producing 50% inhibition at 0.4 ± 0.1 mM. The inhibition was selective for PMCA, since there was no inhibition of the Mg^{2+}-ATPase or the Na^{+}-K^{+}-ATPase of the erythrocyte ghosts or SERCA of skeletal muscle. Caloxin 2A1 also inhibited formation of the acylphosphate from ATP and it produced an endothelium-dependent relaxation in rat aorta (16). These data suggest that extracellular domains play a role in the functioning of PMCA. More importantly, the discovery of caloxin 2A1 will help determine the physiological significance of PMCA in an intact cell.

1.6 *Objectives of this Study*

All of the known functions of PMCA, such as high affinity Ca^{2+}-binding, binding of ATP, acylphosphate formation and hydrolysis and activation by Ca^{2+}-calmodulin, have been assigned to the intracellular or TM domain of the pump (13-15). Yet caloxin 2A1

(caloxin) caused inhibition of PMCA in erythrocyte ghosts even though it is a peptide selected for binding to an extracellular domain of the pump. *AIM I* of this study is to delineate the mechanism of inhibition of the erythrocyte Ca^{2+}-Mg^{2+}-ATPase by caloxin. We hypothesize that caloxin does not compete with the substrates of the pump for binding. *AIM II* of this study is to determine whether the inhibition of PMCA by caloxin is isoform selective. Caloxin was designed for binding to the PED2 sequence of PMCA1. However it caused inhibition of the Ca^{2+}-Mg^{2+} ATPase activity in erythroctyes, which contain mainly PMCA4. Therefore, we hypothesize that caloxin will inhibit all isoforms of PMCA, but perhaps with different affinity.

2.0 MATERIALS AND METHODS

2.1 Materials

^{32}P-γ-ATP and ^{32}P-orthophosphate were obtained from Amersham (Piscataway, NJ). Agar, trypticase peptone and yeast extract were obtained from Becton Dickinson (Cockeysville, MD). Fetal bovine serum was from CanSera (Etobicoke, Ontario). Hygromycin and doxycycline were obtained from Clontech (Palo Alto, CA). G418, glutamine, acrylamide and agarose were obtained from GibcoBRL (Grand Island, NY). Fluo 3 acid was obtained from Molecular Probes (Eugene, OR). 3[N-morpholino]propane sulfonate-NaOH (MOPS), (2-[N-Morpholino]ethanesulfonic acid) (MES), Dulbecco's modified Eagles's medium (DMEM), ampicillin, phenylmethylsulfonyl fluoride (PMSF), ATP, bovine serum albumin (BSA), imidazole, EGTA, ouabain, NADH, phospho(enol)pyruvate (PEP), pyruvate kinase-acetate dehydrogenase, calmodulin (from bovine testes) and tetracycline were obtained from Sigma (St Louis, MO). All other chemicals were purchased from standard commercial sources.

2.1.1 PMCA plasmids

Human PMCA4b and rat PMCA3 in pmm2 expression vectors (pMM2PM4, pMM2PM3) were donated by Dr. Penniston (Mayo Clinic, Rochester, Minnesota). Microsomes isolated from Sf9 cells expressing rat PMCA2b were also donated by Dr. Penniston. Rat PMCA1a in pBR322 expression vector (RB11-1) was donated by Dr. G. Shull (University of Cincinnati, Cincinnati, Ohio).

2.2 Construction of PMCA1 plasmid (pcDNAPM1)

2.2.1 Restriction endonuclease digestion

Full-length PMCA1 gene was excised from RB11-1 plasmid using Bst1107I and BamHI and ligated to pcDNA3.1- vector following its digestion with EcoRV and BamHI. 15 μg of RB11-1 was digested with 30 units of Bst1107I restriction endonuclease in 2x Tango buffer (66 mM Tris-acetate pH 7.9 at 37°C, 20 mM magnesium acetate, 132 mM potassium acetate, 0.1 mg/ml BSA) at 37°C for approximately 2 hours (100 μl final volume). Following heat inactivation of Bst1107I (30 min at 70°C), the sample was diluted to 1x Tango with water and 40 units of BamHI endonuclease was added (200 μl final volume). The digestion reaction proceeded for approximately 2 hours at 37°C and the enzyme was subsequently inactivated (30 min at 70°C). Digestion of pcDNA3.1- proceeded under similar conditions, except the DNA was digested with 30 units EcoRV in 2x OPA buffer (20 mM Tris-acetate pH 7.5, 20 mM magnesium acetate, 100 mM potassium acetate) instead of with Bst1107I in 2x Tango. BamHI digestion occurred in 1x OPA under the same conditions outlined for digestion of RB11-1.

Following each digestion reaction, a small amount of product was separated on a 1.0 % agarose gel to check for complete digestion. Gels were stained with dilute ethidium bromide, destained in water and then exposed to UV light and photographed with a Kodak digital camera.

2.2.2 Dephosphorylation of vector DNA

Digested vector DNA was dephosphorylated prior to gel purification. 0.1 unit of calf intestinal alkaline phosphatase was added to the pcDNA3.1- digestion mixture in the presence of 1X OPA buffer (50 µl final volume) according to the instructions given by the manufacturer. Dephosphorylation proceeded at 37°C for 30 min, followed by heat inactivation at 85°C for 20 min.

2.2.3 Gel purification of digested DNA

Digestion products were separated on 1.0 % agarose gels. The bands were stained with dilute ethidium bromide and then visualized using a Dark Reader. The area of gel containing the fragment to be purified was excised with a clean, sharp blade. The DNA was extracted using the CONCERT Rapid Gel Extraction System (GibcoBRL, Grand Island, NY) according to the manufacturer's instructions. Briefly, the gel was dissolved in solubilization buffer and the agarose removed by passing through a spin cartridge leaving behind the bound DNA. The DNA was washed and then eluted from the filter with warm TE (Tris-EDTA) buffer. The DNA was quantified on 1.0 % agarose gels and then used in ligation reactions.

2.2.4 Ligation reactions

Ligation reactions were performed with T4 DNA Ligase according to the manufacturer's instructions. Briefly, digested and purified vector DNA and insert DNA were mixed in various ratios. 2 µl of 10X ligation buffer (400 mM Tris-HCl, 100 mM $MgCl_2$, 100 mM DTT, 5 mM ATP, pH 7.8 at 25°C) and 1 µl (5 units) of T4 DNA ligase were added and the volume brought up to 20 µl with water. The mixture was incubated overnight at 15°C.

2.2.5 Bacterial transformation

XL2 Blue Ultracompetent Cells (Stratagene, Cedar Creek, TX) were used for transformation of pMM2, pMM2PM4, pMM2PM3, pcDNA3.1- (Invitrogen, Burlington, Ontario), pcDNAPM1, pTREhyg (Clontech, Palo Alto, CA) and pTREPM1. The cells were thawed on ice and β-mercaptoethanol was added to a final concentration of 25 mM. The cells were distributed among 15 ml polypropylene tubes (20 µl/tube) and then 2-5 µl of ligation product was added directly to the cells. This mixture was kept on ice for 45-60 min and then heat shocked at 42°C for 30 sec. The cells were then promptly returned to ice for 2 min. 200 µl of SOC medium (2% trypticase peptone, 0.5 % yeast extract, 10 mM NaCl, 2.5 mM KCl, 20 mM $MgSO_4$, 20 mM glucose) was added and the tubes were incubated for 1 hour at 37°C in a shaker (250 rpm). The cells were diluted in SOC and spread with a sterile spreader on LB Agar (85.6 mM NaCl, 0.5 % yeast extract, 1 % trypticase peptone, 1.5 % agar) plates containing 100 µg/ml ampicillin. The plates were incubated at 37°C overnight and stored at 4°C if required. For transformation of RB11-1 plasmid, XL1-Blue MRF' Kan Supercompetant Cells (Stratagene, Cedar Creek, TX) were

used. The same protocol was followed except the cells were spread on LB Agar plates containing 10 μg/ml tetracycline.

2.2.6 Isolation of plasmid DNA from bacterial cells

EndoFree Plasmid Purification Kits (QIAGEN, Mississauga, Ontario) were used for isolating DNA from bacterial cultures. Briefly, the cells were harvested by centrifugation, resuspended, then lysed in NaOH-SDS buffer and neutralized with acidic potassium acetate buffer. A precipitate containing genomic DNA, proteins, cell debris and SDS was removed by passing the lysate through a filter cartridge provided with the kit. The DNA was washed, eluted from the filter and precipitated with isopropanol. After washing with 70 % ethanol the DNA was air-dried and then dissolved in water or TE. The DNA was quantified on agarose gels or using a spectrophotometer.

2.3 Construction of PMCA1 plasmid (pTREPM1) for incorporation into Tet-Off Gene Expression System

2.3.1 Polymerase chain reaction and restriction endonuclease digestion

The following primers were used to amplify the full-length coding region (74-3896 bp) of PMCA1 from RB11-1 plasmid and create unique restriction sites (BamHI and SalI (in bold)) at each end of the fragment.

BamHI PM74up: 5'-**GGATCCGGATCC**GGCCAGTGGTCAAGATAC-3'

SalI PM3896down: 5'-**GTCGACGTCGAC**GGATGTGCGGCTCTGAAT-3'

PCR was carried out under the following conditions: 25 ng RB11-1 template, 200 μM each of dATP, dCTP, dGTP and dTTP, 1 μM of each primer, 2.5 units of PfuTurbo DNA

Polymerase (Stratagene, Cedar Creek, TX), 1x Pfu buffer (20 mM Tris-HCl, pH 8.8, 2 mM MgSO4, 10 mM KCl, 10 mM $(NH_4)_2SO_4$, 0.1 % Triton X-100, 0.1 mg/ml nuclease-free BSA). Additional $MgSO_4$ was added to make the final $[Mg^{2+}]$ 5 mM. PCR consisted of denaturation at 95°C for 1 min, annealing at 54°C for 1 min and reaction at 72°C for 5 min, for 5 cycles. This was followed by another 20 cycles, except annealing was performed at 72°C. A small amount of the PCR sample was electrophoresed in a 1 % agarose gel to confirm the correct sized product was amplified. The remainder was purified and concentrated using a MinElute PCR Purification Column (GibcoBRL, Grand Island, NY), which removes low molecular weight products, primers, enzyme, salt, etc. After concentrating the product, it was digested with 30 units BamHI in 1X OPA buffer at 37°C for 2 hours. Digestion with 30 units SalI proceeded in 2X OPA buffer at 37°C for 2 hours. The enzymes were inactivated at 65°C for 15 min. The digestion of pTREhyg vector DNA with BamHI and SalI proceeded in a similar manner as that outlined for insert DNA. The products were electrophoresed on 1 % agarose gels. Gel purification, ligation, transformation and isolation of plasmid DNA were performed by the same methods outlined for that of pcDNAPM1 plasmid (see section 2.2).

2.4 Restriction mapping

BclI digestion: Digestion reactions with BclI endonuclease were carried out in 1X Buffer C (10 mM Tris-HCl, 10 mM $MgCl_2$, 50 mM NaCl, 1 mM DTT, pH 7.6 at 50°C) at 50°C for 1 hour.

PvuI digestion: Digestion reactions with PvuI endonuclease were carried out in 1X Buffer D (6 mM Tris-HCl, 6 mM $MgCl_2$, 150 mM NaCl, 1 mM DTT, pH 7.9 at 37°C) at 37°C for 1 hour.

BstEII digestion: Digestion reactions with BstEII endonuclease were carried out in 1X NEBuffer3 (50 mM Tris-HCl, 10 mM $MgCl_2$, 100 mM NaCl, 1 mM DTT, pH 7.9 at 25°C) at 60°C for 1 hour.

PstI digestion: Digestion reactions with PstI endonuclease were carried out in 1X OPA buffer (10 mM Tris-acetate pH 7.5, 10 mM magnesium acetate, 50 mM potassium acetate) at 37°C for 1 hour.

HindIII digestion: Digestion reactions with HindIII endonuclease were carried out in 1X NEBuffer2 (10 mM Tris-HCl, 10 mM $MgCl_2$, 50 mM NaCl, 1 mM DTT, pH 7.9 at 25°C) at 37°C for 1 hour.

2.5 Preparation of human erythrocyte leaky ghosts

Human erythrocyte leaky ghosts were isolated as previously described (42). Briefly, 25-30 ml of human blood in acid citrate dextrose was obtained and centrifuged at 6000 rpm for 5 min to remove the plasma and buffy coat (containing platelets). The lower layer containing the erythrocytes was transferred to four 250 ml bottles. The cells were washed with 10 volumes of 172 mM Tris-HCl pH 7.6 (at 4° C) followed by centrifugation at 5,000 rpm for 5 min and removal of the clear supernatant. This washing step was repeated four times. The cells were then lysed with 14 volumes of chilled water. Following centrifugation at 12,000 rpm for 10 min, the red supernatant was removed, leaving behind a loose and a tight pellet. The pellets were washed with 150 ml

imidazole-EDTA (10 mM imidazole-HCl, 1 mM EDTA, pH 7.0 at 23° C) followed by centrifugation at 12,000 rpm for 10 min and removal of the red supernatant. This washing step was repeated 8-10 times until the liquid and pellet were pale and transparent. The loose pellet was transferred to clean bottles and washed once with 150 ml imidazole-HCl (40 mM imidazole-HCl, pH 7.0 at 23° C). The loose pellets were then pooled into a 50 ml tube and centrifuged a 18,000 rpm for 5 min. This pellet was aliquoted and stored at -80°C until use. An aliquot was used for protein estimation.

2.6 Cell culture

COS-M6 cells were maintained at 37° C in Dulbecco's modified Eagles's medium (DMEM) supplemented with: 0.5 mM HEPES pH 7.4, glutamine (2 mM), gentamicin (50 mg/l), amphotericin B (0.125 mg/l), and 10% FBS. HeLa Tet-Off cells (Clontech) were grown in DMEM supplemented with 0.5 mM HEPES pH 7.4, glutamine (2 mM), 10 % Tet System Approved Fetal Bovine Serum (Clontech). Selection medium also included 100 μg/ml G418 (to maintain incorporation of the regulatory plasmid in these cells), 200 μg/ml hygromycin (to select for cells containing the pTREPM1 or pTRE response plasmid) and 1 μg/ml doxycycline (to keep transcription of PMCA1 turned off).

2.7 Transfections

2.7.1 Choosing a transfection reagent

COS-M6 cells were seeded at a density of 3.5×10^5 cells/well in 6-well plates and grown in DMEM. When the cells were 60-80 % confluent (typically in 24 hours), they were transfected with Enhanced Green Fluorescence Protein (EGFP) (Clontech) using

DMRIE-C (LifeTechnologies, Grand Island, NY), Effectene (Qiagen, Mississauga, Ontario) or FuGENE 6 (Roche, Laval, Quebec) reagents according to the instructions given by the manufacturer. Various ratios of reagent (μl):DNA (μg) were tested and are as follows: DMRIE-C, 3:0.5, 3:1.5, 3:3, 6:1; Effectene, 4:0.4, 10:0.4, 20:0.4; FuGENE, 3:1, 6:1, 12:1. The cells were harvested 24-48 hours post-transfection. Transfection efficiency (percentage of total cell population expressing EGFP) was determined using flow cytometry. All subsequent DNA transfections were carried out using FuGENE 6 reagent.

2.7.2 Transfection of COS-M6 cells using FuGENE

COS-M6 cells were seeded onto 10 cm^2 plates at a density of $1.5x10^6$ cells/plate and transfection was initiated when the cells were 60-80 % confluent. The DNA-FuGENE complex for each plate was prepared by incubating 6 μg of DNA and 36 μl FuGENE 6 reagent in 590 μl of serum-free DMEM for 30 min at room temperature. This mixture was added dropwise to the plates containing 11.5 ml of DMEM. COS-M6 cells were cultured for 24-48 hrs, harvested and used to assay for expression of the cDNA of interest. The transfection efficiency of each experiment was monitored before cell harvest by co-transfecting 1 plate of cells with EGFP and assessing its expression using fluorescence microscopy with a 450-500 nm filter.

2.7.3 Transfection of HeLa Tet-Off cells and selection of double-stable cell lines

Transfection of pTREPM1 and pTRE using FuGENE reagent was initiated when the HeLa cells were 60-80 % confluent according to the method outlined for COS-M6

cells except 100 μg/ml G418 was included in the medium. 24 hours post-transfection, 200 μg/ml hygromycin was added to fresh G418-containing medium to begin selecting for cells containing the pTREPM1 or pTRE response plasmids. The cells were also cultured in the presence of 1μg/ml doxycycline (Dox) to keep transcription of PMCA1 turned "off". This selection medium was replaced every two days. When the cells reached confluence, they were seeded at very low density in the presence of selection medium. Several weeks later, healthy colonies were isolated and transferred to individual plates. Each colony of cells was removed using a small circular sterile filter paper soaked in trypsin-EDTA. The cells were washed free from the filter paper by shaking in selection medium contained in 60 cm^2 dishes. These cells were propagated in selection medium. The cells were typically split 1:10 when they reached confluence.

2.8 Isolation of crude microsomes

Cells were washed twice with cold phosphate-buffered saline (PBS) and harvested by scraping in a buffer containing: 250 mM sucrose, 20 mM MOPS pH 6.8, 1 mM dithiothreitol (DTT), 1 mM EGTA and 0.5 mM phenylmethylsulfonyl fluoride (PMSF). The cells were homogenized using a Polytron (four, 5-s bursts). The homogenate was centrifuged (4°C) in 50 ml tubes at 10,000 rpm for 10 min. The supernatant was filtered through cheesecloth and centrifuged (4°C) at 50,000 rpm for 30 min. The resulting pellet was resuspended in 40 mM imidazole-HCl, pH 7.0, containing 1 mM DTT. An aliquot was used for protein estimation and the remainder was kept on ice until use.

2.9 Protein estimation

Protein estimation was carried out with Bradford Reagent (Bio-Rad, Hercules, CA) using bovine serum albumin to construct the standard curves. Absorbance was measured at 595 nm. The standard curve was fitted and linear regression was performed using the Lotus 1-2-3 computer programme.

2.10 Caloxin synthesis

The screening procedure has been previously described (16). Briefly, caloxin was obtained by screening a random peptide phage display library for binding to the second extracellular domain (residues 401-413) sequence of PMCA1b. The peptide VSNSNWPSFPSSGGG-amide was synthesized and eventually termed caloxin. Randomization of residues in the caloxin peptide gave the sequence SWSSFPGSGGVSNPN-amide and this peptide was synthesized for use as a control.

2.11 Coupled enzyme assay to measure Ca^{2+}-Mg^{2+}-ATPase activity

Erythrocyte leaky ghosts or crude microsomes were mixed with or without caloxin for 30 min on ice before the assay. The Ca^{2+}-Mg^{2+}-ATPase assays were performed at 37°C by monitoring the disappearance of NADH using a fluorometer (excitation at 340 nm and emission at 460 nm) in a coupled enzyme assay described earlier (61, 62). Typically basal Mg^{2+}-ATPase was first determined in a 135 µl solution containing 0.02-0.04 mg protein, 0.1 mM ouabain, 100 mM NaCl, 20 mM KCl, 6 mM $MgCl_2$, 30 mM imidazole-HCl pH 7.0, 0.5 mM EDTA, 0.55 mM NADH, 1 mM phospho(enol)pyruvate, excess pyruvate kinase-acetate dehydrogenase, 0.5 mM ATP, 0.5

mM EGTA and 4 μg/ml calmodulin. 10 μM cyclopiazonic acid (CPA), 5 mM sodium azide and 0.05 % Triton X-100 were also included in this reaction mixture when measuring Ca^{2+}-Mg^{2+}-ATPase activity in crude microsomes. Then, 10 μl of 8 mM $CaCl_2$ was added and the total ATPase activity was determined. The difference between the total ATPase activity and the basal Mg^{2+}-ATPase activity was the Ca^{2+}-Mg^{2+}-ATPase activity. When concentrations of Ca^{2+}, ATP or calmodulin were varied, those of all the other components were kept at the saturating levels indicated above. Using Fluo 3 (Kd for Ca^{2+} at 37°C = 864 nM (53)), a conditional dissociation constant was determined to be 2.2 μM for CaEGTA under the conditions of the assay and this constant was used to determine the concentrations of $CaCl_2$ needed to attain specified concentrations of free Ca^{2+}.

2.12 Western blot analysis

Microsomes were suspended in 4:1 sample buffer consisting of 7.5 % SDS, 25 % glycerol, bromophenol blue, 31.25 % by volume 4X stacking gel buffer pH 6.8 and 1 mM DTT. The microsomal proteins were separated in 1.5 mm thick SDS-polyacrylamide gels according to the method of Laemmli (48). This gel system consisted of two layers: a 5% upper or stacking gel and a 7.5% lower or separating gel differing in their ionic strength and pH. Following electrophoresis, the proteins were electroblotted overnight onto nitrocellulose at 15 volts (10-15° C) according to the method of Towbin et al. (79). Nonspecific protein binding sites were blocked with Blotto (10% non-fat dry milk powder in PBS) and then treated with a 1000X dilution of monoclonal anti-PMCA antibody 5F10 (Affinity BioReagents, Golden, CO) in Blotto for 1.5 hours. 5F10 reacts

with all 4 isoforms of PMCA and recognizes a ~ 140 kDa band. The membrane was then washed several times with PBS and treated with 2500X dilution of anti-mouse horseradish peroxidase-conjugated secondary antibody (Amersham Biosciences, Piscataway, NJ) in Blotto for 1 hour. After washing several times with PBS the primary antibody binding was visualized by enhanced chemiluminescence using the ECL Western Blotting Analysis System (Amersham Biosciences) according to the instructions given by the manufacturer. The molecular weight of the protein band of interest was estimated using RPN 800 Full Range Rainbow protein molecular weight marker (Amersham), which was visible on the membrane after transblotting.

2.13 Acylphosphate assays

The Ca^{2+}-dependent formation of the 140 kDa acid stable acylphosphate intermediate was determined from ^{32}P-γ-ATP and ^{32}P-orthophosphate (33). In either instance the ghosts were incubated first, with or without the peptide, for 30 min at 0°C. For the acylphosphate formation from ATP, the suspensions were then incubated at 0°C with a solution containining imidazole, KCl, $CaCl_2$ and calmodulin before adding the ^{32}P-γ-ATP. The final volume of this reaction mixture was 0.2 ml and following were the concentrations of the various components: 30 mM imidazole-HCl pH 6.8, 100 mM KCl, 0.05 mM $CaCl_2$, 4ug/ml calmodulin, 0.005 mM ATP with trace amounts of ^{32}P-γ-ATP, peptides as specified and ghost protein 0.2 to 0.4 mg/ml. The components were incubated at 0°C for 2 min. The reaction was then quenched with 0.25 ml ice-cold TCAP (10% trichloroacetic acid, 50 mM phosphoric acid) containing 0.5 mM unlabelled ATP and placed on ice for 5 min. The samples were then centrifuged at 4°C, the supernatant

discarded and the pellet washed with 1.25 ml of TCAP. The final pellet was suspended in MEDS buffer pH 5.5 (10 mM MOPS, 1 mM EDTA, 10 % sucrose, 3 % SDS, 10 mM DTT and 0.01 % methyl green) and electrophoresed using SDS-polyacrylamide gels at pH 4.0 as described previously (6). The acylphosphates were quantified using a phosphorimager and Image Quaint Software to determine the intensity of each band. For the acylphosphate formation from orthophosphate, dimethylsulfoxide was added to a final concentration of 32%, the samples incubated for 10 min at 0°C, placed at 22-24 °C and orthophosphate was then added. Typically the final reaction volume was 0.125 ml and had the following composition in mM: 10 EGTA, 5 $MgCl_2$, 50 MES-KOH pH 6.4, 0.05 potassium orthophosphate. After 10 min, the reaction was quenched with 0.25 ml of TCAP, precipitated, washed with TCAP, suspended and electrophoresed in the same manner as for the acylphosphates formed from ATP.

2.14 Data Analysis

Values given are mean ± SEM. Where applicable, Student's t-test was used and values of $p < 0.05$ were considered to be statistically significant. Non-linear regression was used to determine inhibition constant using the software FigP. (Biosoft Corporation, USA).

3.0 RESULTS

Caloxin is a peptide selected for binding to the second extracellular domain sequence of PMCA1 (16). It inhibited selectively, the Ca^{2+}-Mg^{2+}-ATPase activity in erythrocyte leaky ghosts, which contain mainly PMCA4 (16, 75). In the present study we attempted to characterize the mechanism of inhibition of the pump by CALOXIN (***AIM I***) and the effect of CALOXIN on different isoforms of PMCA (***AIM II***).

3.1 *AIM I: mechanism of action of CALOXIN*

All of the known functions of PMCA, such as high affinity Ca^{2+}-binding, binding of ATP, formation of acylphosphate and its hydrolysis and activation by calmodulin are assigned to the intracellular domains of the protein (13-15). However caloxin was designed for binding to an extracellular domain (PED2) of the pump. The mechanism by which extracellular binding of caloxin leads to inhibition of the pump was investigated.

3.1.1 Non-competitive inhibition

Erythrocyte leaky ghosts were used to study the mechanism of inhibition of PMCA by caloxin. An advantage of using human erythrocyte ghosts is that they contain low levels of ecto Mg^{2+}-ATPases and they lack intracellular organelles (eliminating ATPase activity of the SERCA pump), thus decreasing these sources of interference (42). Furthermore, erythrocyte ghosts were made leaky, allowing access to substrates, which bind the pump intracellularly. Since caloxin is designed to bind extracellularly, we tested the hypothesis that caloxin does not compete with the substrates of the PMCA pump for

binding. Equations 1 and 2 describe competitive and non-competitive inhibition, respectively.

$v = Vmax[S]/([S]+Km(1+[I]/Ki))$ 1

$v = (Vmax/(1+[I]/Ki))[S]/([S]+Km)$ 2

where v is the initial velocity of the reaction, Vmax is the maximum velocity, [S] is the substrate concentration, Km is the Michaelis-Menten constant, [I] is the inhibitor concentration and Ki is the inhibition constant. Thus a greater percent inhibition at a non-saturating (near Km) concentration than at a saturating (>>Km) concentration of the substrate indicates competitive inhibition, whereas no difference in the percent inhibition between the two indicates non-competitive inhibition. As the inhibition constant of caloxin is 0.4 ± 0.1 mM in erythrocyte ghosts (16), it becomes prohibitively expensive to run elaborate experiments with a large number of data points. Hence, we have taken the following approach to test our hypothesis: we determined the substrate concentration dependence of the Ca^{2+}-Mg^{2+}-ATPase for Ca^{2+}, ATP and calmodulin, and then compared the effect of 1.87 mM caloxin on a saturating and non-saturating concentration of each substrate. This concentration of caloxin was chosen since it is well above the reported inhibition constant of caloxin for erythrocyte ghosts (16). Ca^{2+}-concentration dependence of Ca^{2+}-Mg^{2+}-ATPase (Fig. 3A) indicates that the pump has a Km of 6 ± 2 μM for Ca^{2+}. Caloxin inhibits this activity at 5 and 53.6 μM Ca^{2+}, as shown in Fig 3B. Fig. 3C shows that the inhibition is not competitive with respect to Ca^{2+}, since the percent inhibition at non-saturating [Ca^{2+}] (55 ± 6 % at 5 μM) does not differ significantly from that at saturating [Ca^{2+}] (64 ± 4 % at 53.6 μM) ($P > 0.05$).

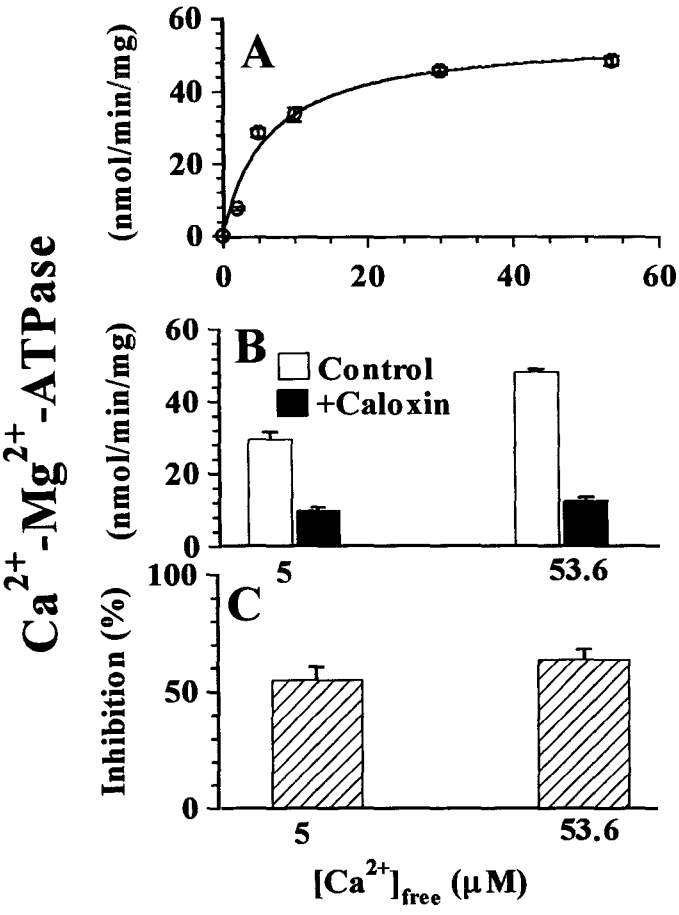

Fig. 3: Free $[Ca^{2+}]$-dependence of Ca^{2+}-Mg^{2+}-ATPase and inhibition by caloxin. A) Free $[Ca^{2+}]$-dependence. Values are mean ± SEM of 3 replicates within one experiment. The experiment was repeated 2 more times. The data fit best with a Km value of 6 ± 2 μM (mean ± SEM) for free $[Ca^{2+}]$. B) Effect of 1.87 mM caloxin on Ca^{2+}-Mg^{2+}-ATPase activity monitored at low (5 μM) and saturating (53.6 μM) free $[Ca^{2+}]$. Values are mean ± SEM of 3 replicates within one experiment. C) Percent inhibition by 1.87 mM caloxin at 5 and 53.6 μM free Ca^{2+} determined from data from 3 experiments on different days such as the one shown in B. Values are mean ± SEM. The percent inhibition values did not differ significantly at the two free Ca^{2+} concentrations ($p > 0.05$).

Fig. 4A shows that the enzyme has a Km of 110 ± 16 μM for ATP. Caloxin inhibits the activity of the pump at 50 and 500 μM ATP (Fig. 4B). Fig. 4C reveals that the inhibition is not competitive with respect to ATP because the percent inhibition at the non-saturating [ATP] (81 ± 3 % at 50 μM) does not differ significantly from that at saturating [ATP] (76 ± 4 % at 500 μM) ($P > 0.05$). Fig. 5A shows that the Ca^{2+}-Mg^{2+}-ATPase has a basal activity in the presence of ATP and Ca^{2+}, and is also activated by calmodulin with 50% of the maximum activation occurring at 12 ± 2 nM. Fig. 5B illustrates the effects of caloxin on the calmodulin-stimulated component of the Ca^{2+}-Mg^{2+}-ATPase. Fig. 5C shows that the inhibition is not competitive with respect to calmodulin since the percent inhibition at the non-saturating [calmodulin] (78 ± 5% at 5.9 nM) does not differ significantly from that at saturating [calmodulin] (80 ± 3% at 235 nM) ($P > 0.05$).

3.1.2 Effect of caloxin on acylphosphate formation from ATP and orthophosphate

In its forward reaction cycle, the PMCA forms a labelled acid-stable phosphorylated intermediate (acylphosphate) from ^{32}P-γ-ATP in the presence of Ca^{2+} (3, 13, 49). Thus the acylphosphate formation requires high affinity Ca^{2+}-binding, ATP-binding and transfer of the gamma phosphate of ATP to the conserved apartic acid residue in the catalytic domain of the pump (see Fig. 1). Inhibition of any of these steps would decrease acylphosphate formation starting from ATP. In the last step of the reaction cycle, this acylphosphate is hydrolysed. However, the last step can be followed in its reverse direction as formation of acylphosphate from labelled orthophosphate at the same residue, in the low affinity conformation of the enzyme (see Fig. 1).

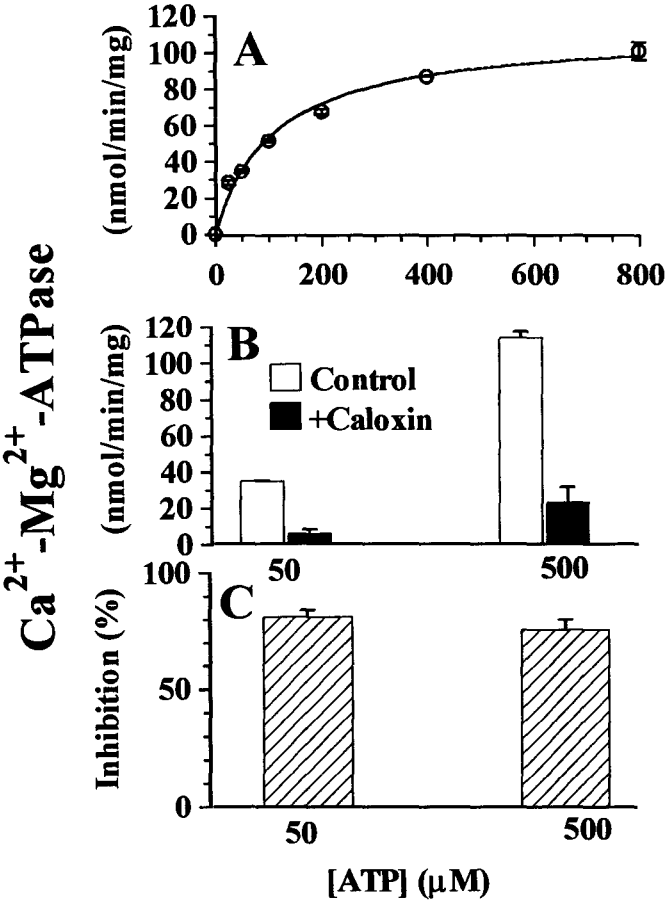

Fig. 4: [ATP]-dependence of Ca^{2+}-Mg^{2+}-ATPase and inhibition by caloxin. A) [ATP]-dependence. Values are mean ± SEM of 2 replicates within one experiment. This experiment was repeated 2 more times. The data fit best with a Km value of 110 ± 16 μM (mean ± SEM) for ATP. B) Effect of 1.87 mM caloxin on Ca^{2+}-Mg^{2+}-ATPase monitored at low (50 μM) and saturating (500 μM) ATP. Values are mean ± SEM of 3 replicates within one experiment. C) Percent inhibition by 1.87 mM caloxin at 50 and 500 μM ATP determined from data from 3 experiments on different days such as the one shown in B. Values are mean ± SEM. The percent inhibition values did not differ significantly at the two ATP concentrations ($p > 0.05$). Note that these experiments were carried out in the presence of excess (6 mM) $MgCl_2$ and the value of ATP reflects the total ATP.

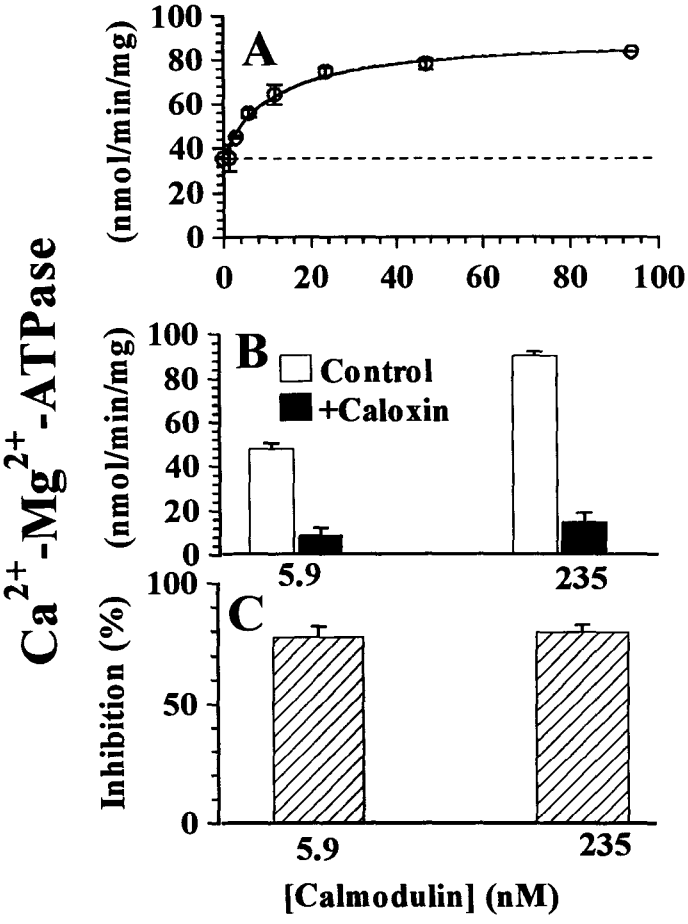

Fig. 5: Calmodulin activation of Ca^{2+}-Mg^{2+}-ATPase and inhibition by caloxin. A) [calmodulin]- dependence. Values are mean ± SEM of 3 replicates within one experiment. The experiment was repeated 2 more times. Dotted line shows the activity without calmodulin. Calmodulin activation data fitted best with a Ka value of 12 ± 2 nM (mean ± SEM) for calmodulin. B) Effect of 1.87 mM caloxin on Ca^{2+}-Mg^{2+}-ATPase monitored at low (5.9 nM) and saturating (235 nM) calmodulin. Values are mean ± SEM of 3 replicates within one experiment. C) Percent inhibition by 1.87 mM caloxin at 5.9 and 235 nM calmodulin determined from data from 3 experiments on different days such as the one shown in B. Values are mean ± SEM. The percent inhibition values did not differ significantly at the two calmodulin concentrations ($p > 0.05$).

However, the reverse reaction does not require Ca^{2+}-binding or the hydrolysis of ATP, just the formation of the covalent bond. In fact, this reaction is inhibited by Ca^{2+} (17). Therefore, the two acylphosphates are formed from two separate conformations of the Ca^{2+}-Mg^{2+}-ATPase (E1 and E2). Fig. 6A (lane 1) shows that under the reaction conditions outlined in the Materials & Methods section, a single 140 kD phosphorylated intermediate was formed from ^{32}P-ATP (forward reaction). During gel electrophoresis, it migrated above the 110 kD phosphorylated SERCA pump intermediate which was used as a marker (not shown). The 140 kD acylphosphate was formed in the presence of Ca^{2+} but not in its absence (Fig. 6A lane 2). Next, we tested the effect of 3.4 mM caloxin on the reaction cycle of the pump. The acylphosphate formation in the forward reaction was inhibited by caloxin (Fig. 6A lane 3). This figure also shows that the sequence of caloxin is needed to cause the inhibition and not just the amino acid composition, because a randomized peptide with the same amino acid composition does not produce inhibition (Fig. 6A lane 4). In the reverse reaction however, the acylphosphate formation occurs only in the absence of Ca^{2+}, which inhibits this reaction (Fig. 6B lanes 5 and 7). In contrast to the forward reaction, the acylphosphate formation in the reverse reaction is not affected by caloxin and as anticipated the random peptide has no effect (Fig. 6B lanes 6 and 8).

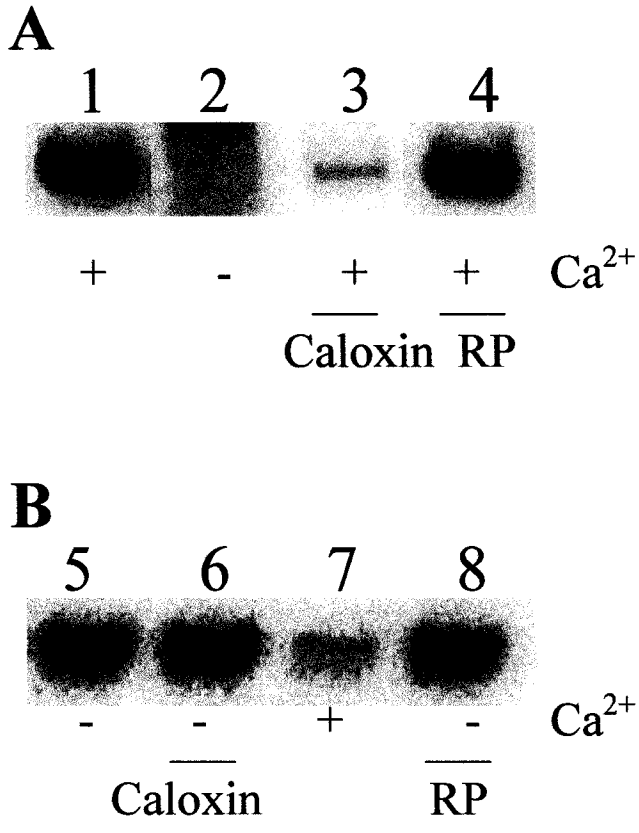

Fig. 6: Effects of caloxin on formation of 140 kDa acylphosphate intermediate. Erythrocyte ghost suspensions were treated with or without 3.4 mM caloxin or random peptide (RP). A) Acylphosphate formation from ^{32}P-γ-ATP. The reaction mixture contained 0.05 mM $CaCl_2$ ($+Ca^{2+}$) or 0.25 mM EGTA ($-Ca^{2+}$). B) Acylphosphate formation from ^{32}P-orthophosphate. The reaction mixture contained 10 mM EGTA ($-Ca^{2+}$) or 1 mM $CaCl_2$ ($+Ca^{2+}$). The position of the bands was verified using the SERCA2b pump acylphosphate (110 kDa) which migrated slightly faster than the PMCA pump (140 kDa). See Materials and Methods for details.

3.2 *AIM II: effect of CALOXIN on different isoforms of PMCA*

Caloxin was selected for binding to the second extracellular domain (PED2) sequence of PMCA1 (16). Yet caloxin inhibits the Ca^{2+}-Mg^{2+} ATPase activity in erythrocyte leaky ghosts, even though erythrocytes contain mainly PMCA4 (and some PMCA1) (16, 75). Due to the homology between the different isoforms in PED2 (Fig. 2), we tested the hypothesis that caloxin would inhibit all isoforms of PMCA, but perhaps with different affinity. Since caloxin was made against the PED2 sequence of PMCA1, caloxin will likely have the highest affinity for PMCA1. To study this, transfection procedures were used to overexpress different isoforms of PMCA in mammalian cells. Typically, microsomes were generated from these cells and used to measure the Ca^{2+}-Mg^{2+} ATPase activity (by a coupled enzyme assay) and abundance of PMCA protein (assessed using Western blot).

3.2.1 Optimizing the Procedures for Studying PMCA activity

3.2.1.1 Optimization of transient transfection procedures

PMCA is a low abundance protein in most tissues, representing less than 0.1% of total membrane protein (13). Furthermore, most tissues contain more than one isoform of the PMCA pump (74). To overcome these obstacles, we undertook the overexpression of specific PMCA isoforms using recombinant expression vectors. The appropriate plasmid of interest was introduced into COS-M6 cells using a transient transfection procedure. COS-M6 cells were chosen since the first report of overexpression of the pump (PMCA4) in mammalian cells was performed in COS cells (1). Secondly, COS-M6 cells responded well to previous attempts at transfection in our lab.

The single most important factor when optimizing transfection efficiency is selecting the proper transfection protocol for your cells (5). Several transfection reagents were first tested for their ability to incorporate and express enhanced green fluorescence protein (EGFP) into COS-M6 cells. EGFP is a reporter system that, when expressed in cells and illuminated by blue or UV light, yields a bright green fluorescence (Clontech Living Colors User Manual). We tested Fugene (Roche), DMRIE-C (Life Technologies) and Effectene (Qiagen) reagents. The transfection reagent:DNA ratio is known to influence the transfection efficiency, hence this parameter was optimized for each of the three reagents. The percentage of cells expressing EGFP (a measure of transfection efficiency) 24-48 hours post-transfection was determined using flow cytometry. The transfection efficiency achieved using Fugene (46 - 57 %) was significantly higher than that of DMRIE-C (20 - 35 %) or Effectene (10 - 28 %). Therefore, Fugene was chosen as the transfection reagent for use in subsequent transfection procedures with PMCAs, at a Fugene:DNA ratio of 6:1.

3.2.1.2 Optimization of the coupled enzyme assay for studying Ca^{2+}-Mg^{2+} ATPase

The coupled enzyme assay for measuring Ca^{2+}-Mg^{2+} ATPase activity used for AIM I had to be optimized for use with COS-M6 microsomes. Microsomes isolated from COS-M6 cells overexpressing PMCA4 were used to optimize the assay since a PMCA4 plasmid was available and its overexpression, compared to other isoforms of the pump, has been well documented in COS cells (1, 36, 65). We were also successful at expressing this plasmid in COS cells, as assessed by Western blot analysis (see Section 3.2.2.1 for details). Unlike erythrocytes, COS-M6 cells contain the SERCA pump as well

as high levels of ecto Mg^{2+}-ATPases. Cyclopiazonic acid (CPA) was included in the reaction solution to inhibit the SERCA pump. The detergent Triton X-100 was incorporated to inhibit ecto Mg^{2+}-ATPases and to solubilize the microsomes, making them leaky to the substrates of the PMCA pump (1, 36). Initially, the microsomes were preincubated with the detergent (0.05 %). However, this introduced large variability since it was difficult to control the length of time the microsomes were exposed to the detergent. Also, when the microsomes were added to the cuvette along with the other reaction components, the detergent was diluted, questioning its effectiveness during the assay. Therefore, we decided not to pre-incubate the microsomes and instead, to include the detergent (0.05 % final) as part of the reaction buffer. The coupled enzyme assay was also optimized for protein and NADH concentrations. Since we wanted to determine the initial velocities, we chose concentrations of protein and NADH at which only a small fraction of NADH was consumed. Typically, 0.55 mM NADH and 15-20 μg of protein were included in each assay.

3.2.2 Effects of CALOXIN on different isoforms of PMCA

3.2.2.1 Isoform 4 of PMCA

3.2.2.1.1 PMCA4 plasmid: A plasmid incorporating human PMCA4b cDNA into pMM2 expression vector was donated from Dr. Penniston's group (pMM2PM4). Restriction digest analysis was performed to determine the nature of this plasmid. The plasmid DNA was cleaved individually with BclI (cuts PMCA4 twice but does not cut pMM2) and PvuI (cuts pMM2 twice but does not cut PMCA4) and the resulting products

were separated by agarose electrophoresis. BclI generated the expected sized fragments (2.2 and 6.6 kb fragments), as did PvuI (0.9 and 7.9 kb fragments).

3.2.2.1.2 Western blot analysis: COS-M6 cells were transiently transfected with pMM2PM4. 48 hours post-transfection, cells were harvested and crude microsomes were prepared. The level of overexpression of PMCA compared to untransfected COS-M6 cell microsomes was estimated by Western blot analysis using monoclonal anti-PMCA antibody (5F10), an antibody that recognizes all isoforms of PMCA (Fig. 7). In the untransfected samples, antibody 5F10 reacted with a band of 140 kDa, the expected size of PMCA (Fig. 7, lanes 1-3). The intensity of the band increased when the cells were transfected with pMM2PM4 (Fig. 7, lanes 4-6). Since the intensity of the bands in lane 3 (5 μg, untransfected) versus lane 6 (1 μg, transfected) are similar, PMCA4 transfected microsomes had approximately 5x the amount of PMCA, suggesting that PMCA4 was overexpressed in these cells.

3.2.2.1.3 Ca^{2+}-Mg^{2+} ATPase activity of PMCA4: To investigate whether the expressed PMCA4 was functional, we measured the Ca^{2+}-Mg^{2+} ATPase activity in membranes from PMCA4 transfected and mock transfected cells using the coupled enzyme assay described in Materials & Methods. COS-M6 cells were transiently transfected with pMM2PM4 or pMM2 (mock transfected). 48 hours later, cells were harvested and crude microsomes were prepared. In 5 separate experiments, the Ca^{2+}-Mg^{2+} ATPase activity of the mock transfected microsomes was significantly lower than that of PMCA4 transfected microsomes ($p<0.05$). After pooling these results, the Ca^{2+}-Mg^{2+} ATPase

activity of mock transfected microsomes was less than 7.7 ± 1.5 % of the Ca^{2+}-Mg^{2+} ATPase activity of transfected samples, suggesting that PMCA4 was overexpressed and was functional in the pMM2PM4 transfected cells.

3.2.2.1.4 Effect of CALOXIN on PMCA4 activity: Having established the functional overexpression of PMCA4, the effect of caloxin was tested on its activity. Fig. 8 shows the inhibition of Ca^{2+}-Mg^{2+}-ATPase in PMCA4 transfected microsomes at various concentrations of caloxin. For each experiment, the values obtained in the presence of caloxin were expressed as a percentage of the control mean on that day and subsequently converted to percent inhibition. Data from several experiments performed on different days (using different microsome preparations), were pooled. The effect of 0, 0.47, 0.94 and 1.87 mM caloxin was determined. These concentrations produced 0, 27 ± 7%, 44 ± 3% and 55 ± 3% inhibition respectively. Using these data points and assuming 100% inhibition, caloxin has an inhibition constant (Ki) of 1.3 ± 0.1 mM for PMCA4.

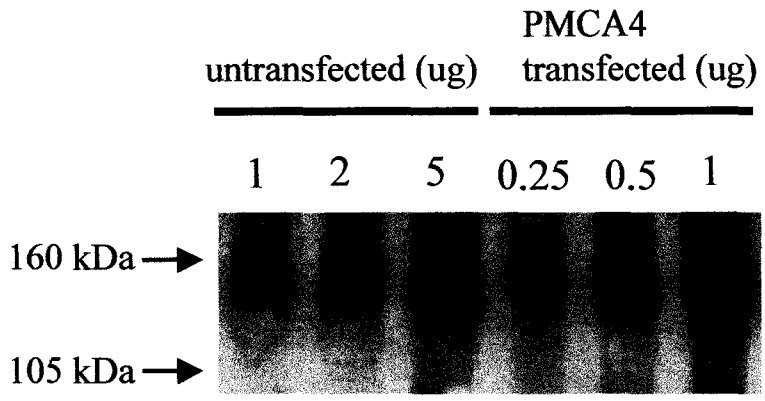

Fig. 7: PMCA4 overexpression detected by Western blot. COS-M6 cells were transfected with pMM2PM4. 48 hours later, cells were harvested and crude microsomes prepared. 0.25, 0.5 or 1 μg of this protein was separated on an SDS polyacrylamide gel, transferred onto nitrocellulose and blotted with anti-PMCA antibody (5F10). 1, 2 and 5 μg of protein from untransfected COS-M6 cells was used as control. The band at 140 kDa is attributed to PMCA.

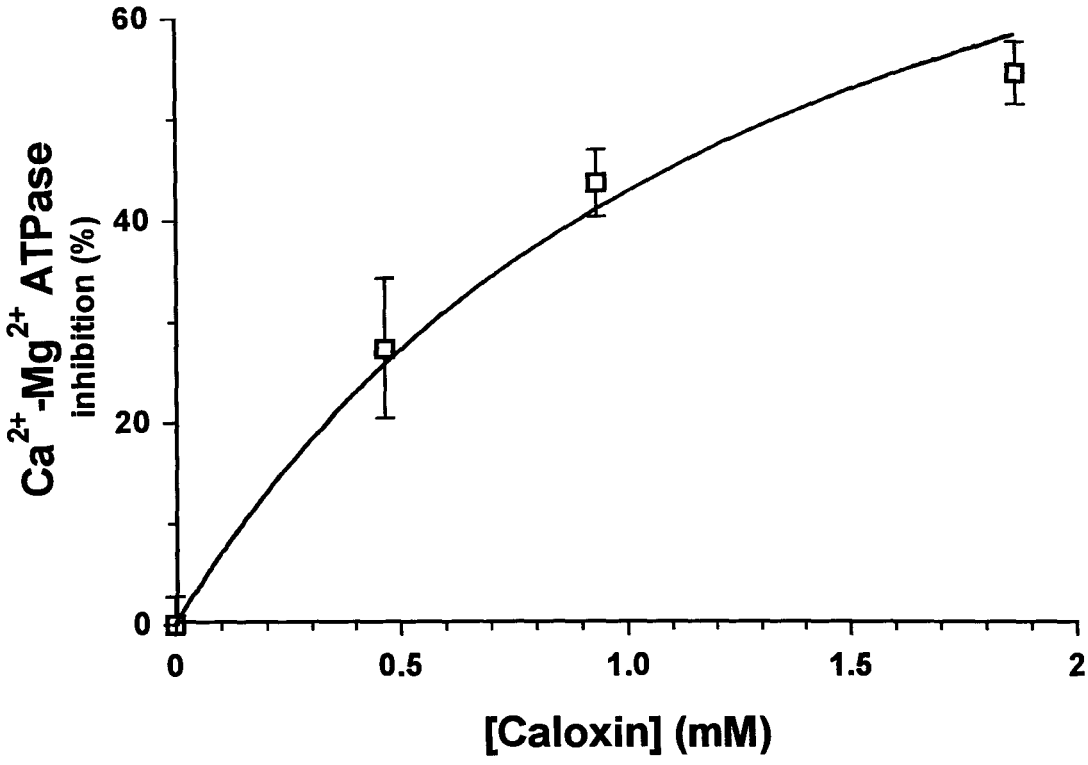

Fig. 8: [Caloxin]-dependence of the Ca^{2+}-Mg^{2+} ATPase in PMCA4 transfected microsomes. COS-M6 cells were transiently transfected with pMM2PM4. 48 hours later, crude microsomes were generated from these cells and the effect of 0.47, 0.94 and 1.87 mM caloxin on the Ca^{2+}-Mg^{2+} ATPase activity was determined using the coupled enzyme assay. Values are expressed as percent inhibition of the control mean ± SEM and represent pooled data from several experiments performed on different days. For 0 mM caloxin, n=18; 0.47 mM, n=7; 0.94 mM, n=13 and 1.87 mM, n=14. Using Michaelis-Menton kinetics and assuming 100% inhibition, Ki = 1.3 ± 0.1 mM.

3.2.2.2 *Isoform 2* of PMCA

3.2.2.2.1 Effect of CALOXIN on PMCA2 activity: Reports on the overexpression of PMCA2 in mammalian cells is limited. Overexpression of PMCA2 using baculovirus-mediated expression in Sf9 cells has been more favorable (67). A limited amount of microsomes made from these cells were donated by Dr. Penniston's group. Thus we were able to test only one concentration of caloxin on the Ca^{2+}-Mg^{2+}-ATPase activity of these microsomes using the coupled enzyme assay (Fig. 9). We tested 1.87 mM caloxin since this was well above the inhibition constant reported for erythrocyte ghosts. Caloxin inhibits PMCA2 pump activity, producing 59.8 ± 4.9 % inhibition at a concentration of 1.87 mM.

3.2.2.3 *Isoform 3* of PMCA

3.2.2.3.1 Ca^{2+}-Mg^{2+} ATPase activity of PMCA3: In preliminary experiments using a PMCA3 plasmid (pMM2PM3) obtained from Dr Penniston's group, we could not reproducibly detect functional overexpression of PMCA3 in COS-M6 cells using the coupled enzyme assay. In only 1 out of 3 experiments, the Ca^{2+}-Mg^{2+}-ATPase activity in PMCA3 transfected microsomes was elevated (61 ± 12 nmol/min/mg) compared to that of untransfected microsomes (12 nmol/min/mg). Our collaborators also reported difficulties overexpressing PMCA3 in the COS cell system, but were unable to provide us with microsomes made from Sf9 cells overexpressing PMCA3 (personal communication).

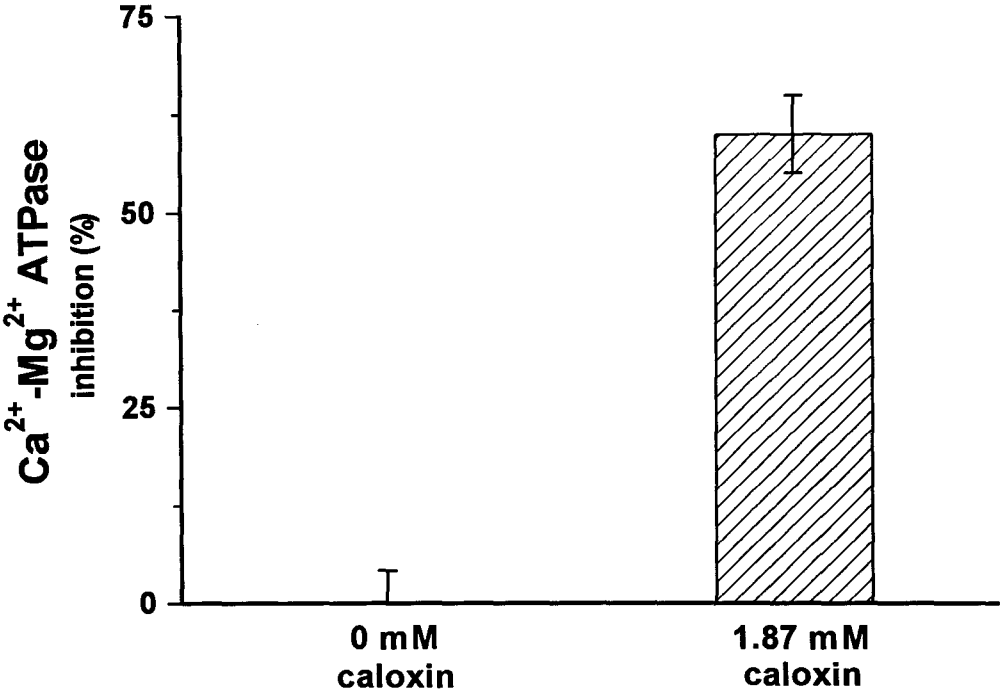

Fig. 9: Effect of caloxin on Ca^{2+}-Mg^{2+} ATPase activity in PMCA2 transfected microsomes. Microsomes generated from Sf9 insect cells expressing PMCA2 were used to test the effect of 1.87 mM caloxin on the Ca^{2+}-Mg^{2+} ATPase activity. Values are expressed as percent inhibition of the control mean ± SEM and represent pooled data from 3 separate experiments.

3.2.2.4 *Isoform 1* of PMCA

Caloxin inhibits the Ca^{2+}-Mg^{2+}-ATPase activity in erythrocyte ghosts with low affinity (Ki of 0.4 ± 0.1 mM) for the pump (16). Caloxin was selected for binding to the PED2 sequence of PMCA1, which may explain its low affinity for erythrocytes since erythrocytes contain mainly PMCA4 (and some PMCA1) (74, 75). Although the amino acid sequence of PMCA1 is similar to that of PMCA4 in this region (except for alanine at position 406 in PMCA1 vs proline in PMCA4), caloxin may represent an isoform selective inhibitor of the PMCA. Therefore, it was important to obtain a cell system overexpressing PMCA1, which could be used to determine the affinity of this isoform for caloxin.

3.2.2.4.1 PMCA1 plasmid: Full-length PMCA1, which had been cloned from a rat brain cDNA library using an oligonucleotide probe derived from a conserved amino acid sequence of the ATP binding site of the P-type ATPases, was obtained from another lab (72). It is designated RB11-1 (in pBR322 vector) and contains a PMCA cDNA insert that has an open reading frame encoding 1,176 amino acids. This would correspond to a 130 kD protein. Surprisingly, since its isolation, there have been only a few reports of PMCA1 overexpression in mammalian cells, but the plasmids used in these experiments were unavailable to us (personal communication) (40, 50). Therefore, we designed a PMCA1 plasmid that could be overexpressed in mammalian cells. The strategy for its design is outlined in Fig. 10. The first step in the construction was to excise the sequence from RB11-1 corresponding to the full-length coding region of PMCA1a.

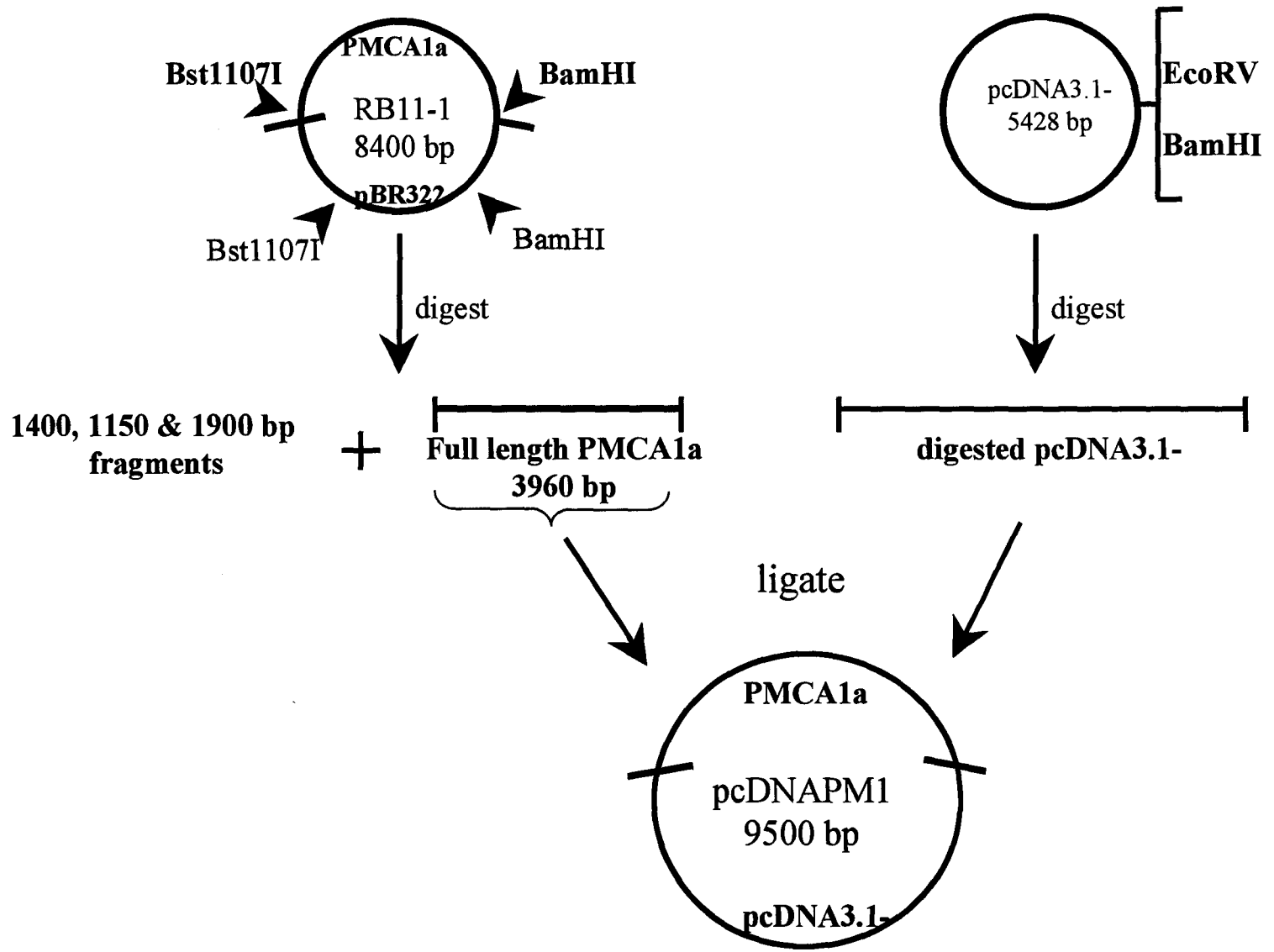

Fig. 10: Strategy for design of pcDNAPM1 plasmid.

To achieve this, RB11-1 was digested first with Bst1107I and then with BamHI to obtain a ~ 4 kb fragment. This fragment was ligated to the pcDNA3.1- expression vector that had been digested with EcoRV and BamHI. Following ligation and transformation, several DNA clones were obtained. Restriction digest analysis was performed on these clones to determine the nature of the DNA. The plasmid DNA was cleaved individually with BstEII (cuts PMCA1 once, but does not cut pcDNA3.1-) and PstI (cuts pcDNA3.1- twice, but does not cut PMCA1) and the resulting products were separated by agarose electrophoresis. These enzymes generated the expected sized fragments (see Fig. 11). Partial sequencing of one of the clones confirmed that PMCA1 had been ligated to pcDNA3.1. This plasmid, termed pcDNAPM1, was used in subsequent experiments.

3.2.2.4.2 Western blot analysis: COS-M6 cells were transiently transfected with pcDNAPM1 or pcDNA3.1- (mock transfected). 48 hours post-transfection, cells were harvested and crude microsomes were prepared. The level of overexpression of PMCA was estimated by Western blot analysis (Fig. 12). Monoclonal antibody 5F10 was used to detect the overexpression of PMCA1. Even when plasmid without insert (mock) was used for transfection, antibody 5F10 reacted with a band of 140 kDa, the expected size of the PMCA (Fig. 12, lanes 1-2). The intensity of the band increased when the cells were transfected with pcDNAPM1 (Fig. 12, lanes 3-4) suggesting that PMCA1 was expressed in these cells.

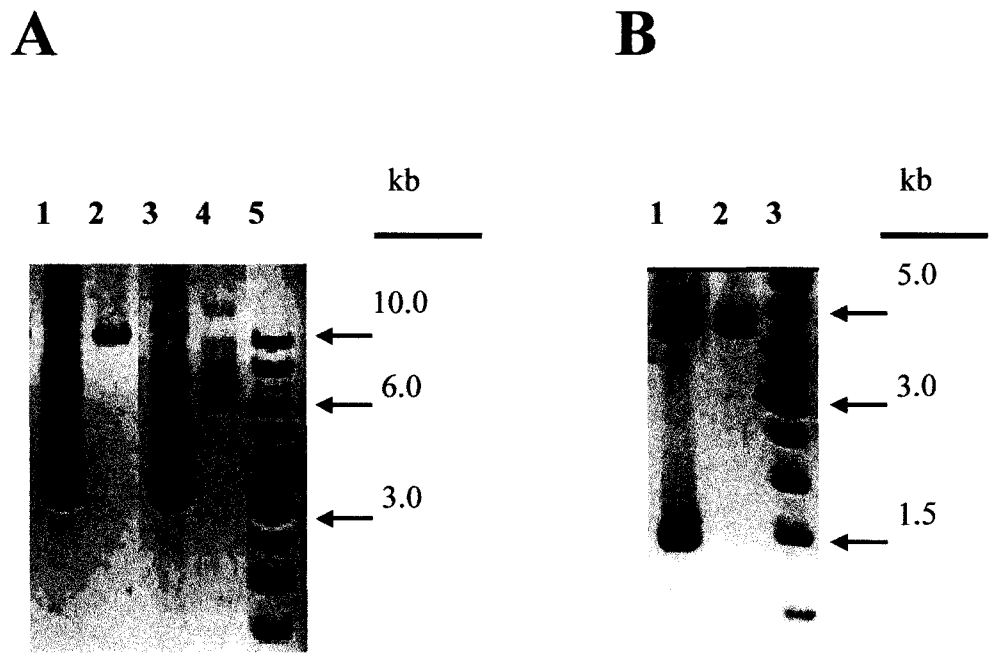

Fig. 11: Restriction digest analysis of pcDNAPM1 plasmid. A) Lane 1, digestion of pcDNA (no insert) with BstEII; lane 2, digestion of pcDNAPM1 with BstEII generated a linear 9.4 kb fragment; lane 3, uncut pcDNA (no insert); lane 4, uncut pcDNAPM1; lane 5, 1kb DNA ladder. B) Lane 1, digestion of pcDNA (no insert) with PstI generated 1.4 and 4.0 kb fragments; lane 2, digestion of pcDNAPM1 with PstI generated 4.8 and 4.5 kb fragments; lane 3, 1 kb DNA ladder.

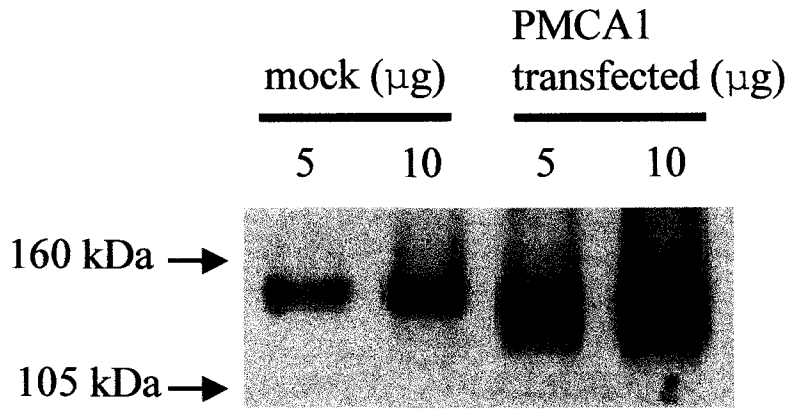

Fig. 12: PMCA1 overexpression detected by Western blot. COS-M6 cells were transiently transfected with pcDNAPM1 or pcDNA3.1- (mock transfected). 48 hours later,cells were harvested and crude microsomes prepared. 5 and 10 μg of each sample were separated on an SDS polyacrylamide gel, transferred onto nitrocellulose and blotted with anti-PMCA antibody (5F10). The band at 140 kDa is attributed to PMCA.

3.2.2.4.3 Ca^{2+}-Mg^{2+} ATPase activity of PMCA1: In order to investigate whether or not the overexpressed PMCA1 was functional, we measured the Ca^{2+}-Mg^{2+} ATPase activity in membranes from PMCA1 transfected and untransfected COS-M6 cells using the coupled enzyme assay described in Materials & Methods. In 3 separate experiments, we could not detect functional overexpression of PMCA1 using the coupled enzyme assay. The transfected microsomes had very low Ca^{2+}-Mg^{2+} ATPase activity. For example, in one experiment the Ca^{2+}-Mg^{2+} ATPase activity of PMCA1 transfected microsomes was 9.0 ± 4.5 nmol/min/mg, which was not significantly different from the enzyme activity of untransfected microsomes (6.5 nmol/min/mg).

3.2.2.4.4 Tet-Off Gene Expression System for PMCA1 overexpression: Next, we tested the hypothesis that the level of PMCA1 overexpression attained with transient transfection was too low to be detected functionally by our coupled enzyme assay. Therefore, we decided to take advantage of the Tet-Off Gene Expression System (Clontech, Palo Alto, CA), which allows for regulated, high-level gene expression. In the Tet-Off system, gene expression is turned on when tetracycline (Tc) or doxycycline (Dox; a Tc derivative) is removed from the culture medium. Induction levels up to 10,000-fold have been observed, making this a very attractive system (Clontech Manual).

Setting up a functional Tet system requires creating a double-stable Tet cell line that contains both a regulatory and a response plasmid. A premade Tet-Off cell line, which already stably expresses the regulatory plasmid was purchased. The response plasmid (pTREhyg) expressing the gene of interest (in our case, PMCA1) had to be constructed. The strategy for its design is outlined in Fig. 13.

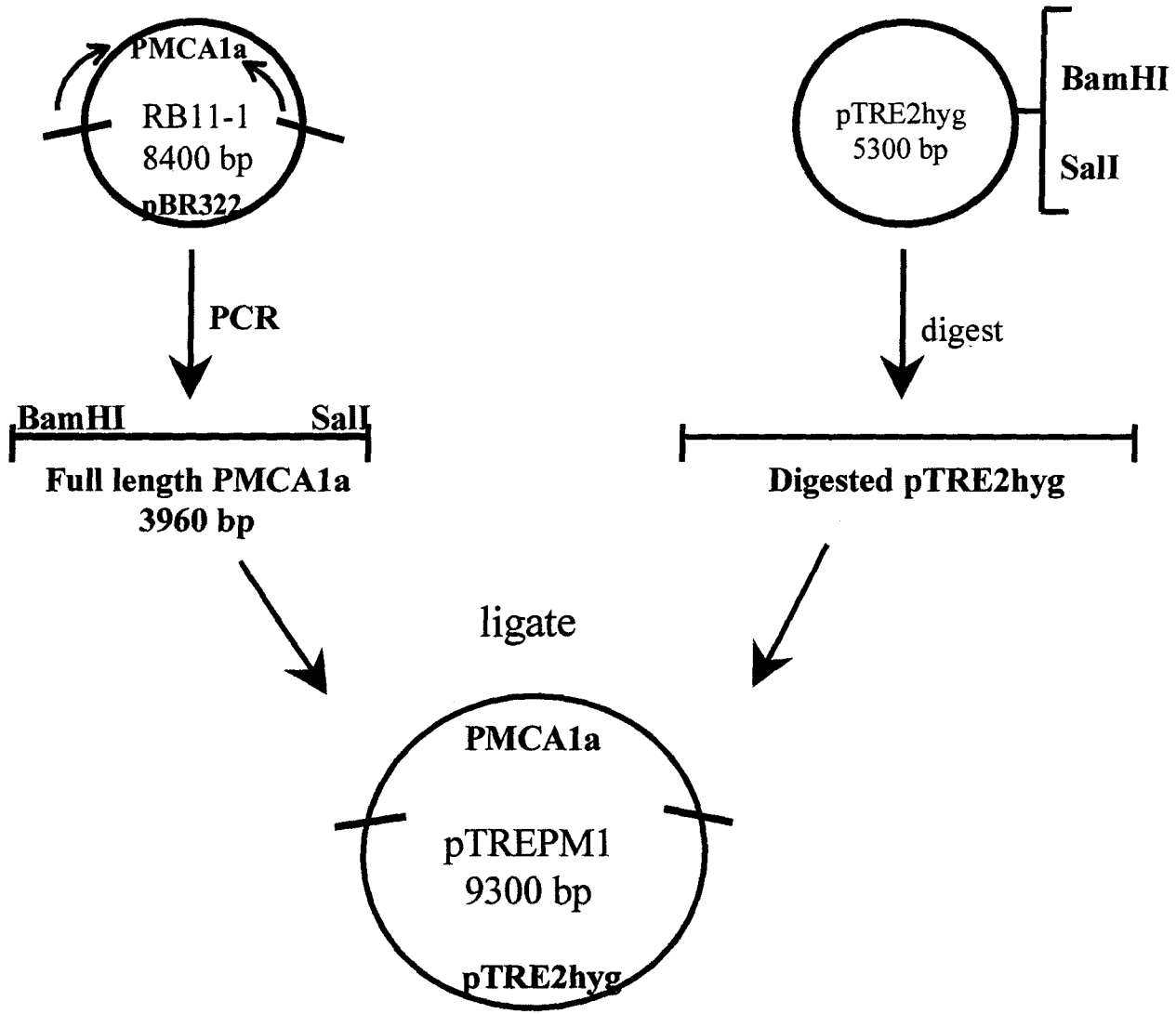

Fig. 13: Strategy for design of pTREPM1 plasmid.

The first step in the construction was to amplify, by PCR, the sequence corresponding to the full-length coding region of PMCA1a (74 - 3896 bp) using RB11-1 as the template DNA. Pfu Turbo DNA polymerase (Stratagene, Cedar Creek, TX) was used in the PCR reaction because of its high fidelity and processivity. This strategy was used instead of restriction digest since the cloning sites available in the pTREhyg vector were incompatible with those in the parent plasmid (RB11-1). Therefore, PCR primers were designed to create unique restriction sites (BamHI and SalI) at each end of the PMCA1 PCR fragment. After obtaining the correct sized PMCA1 fragment (~ 4 kb), it was digested with BamHI and SalI, then ligated to the pTRE2hyg (5.3 kb) expression vector that had also been digested with BamHI and SalI. Following ligation and transformation, we isolated several clones. Restriction digest analysis was performed to determine the nature of the DNA. The plasmid DNA was cleaved individually with PstI and HindIII and the resulting products were separated by agarose electrophoresis. The pTREhyg vector and the PMCA1 insert have one site for each of these enzymes. Digestion of the pTREPM1 plasmid with PstI generated the expected sized fragments (1.5 and 7.6 kb fragments), as did HindIII (3.3 and 5.8 kb fragments). Fig. 14 shows gel pictures of the restriction enzyme digest. Using overlapping primers we sequenced the full-length PMCA1a and the regions of pTRE2hyg vector flanking it. The entire sequence matched that reported for PMCA1a (accession J03753). We called this plasmid pTREPM1.

Clontech offers several Tet-Off cell lines that already stably express the regulatory plasmid. Initially, COS-7 Tet-Off cells were chosen since 1) Clontech reported relatively high levels of induction with these cells (290 ± 40 fold induction) and 2) we used COS cells to test the effect of caloxin on PMCA4 isoform. Unfortunately, the

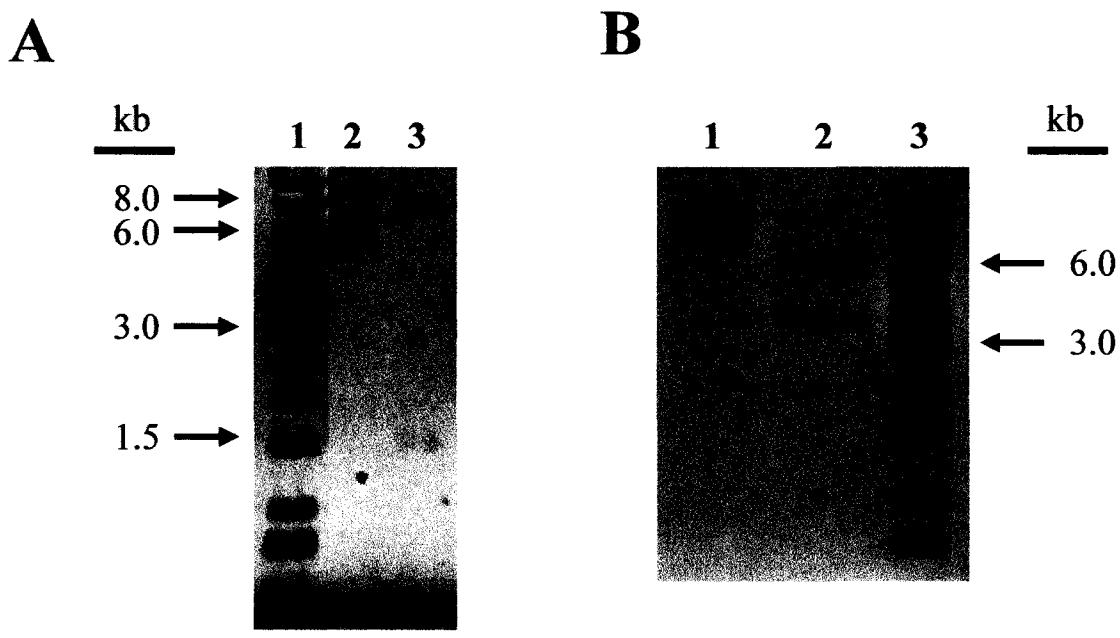

Fig. 14: Restriction digest analysis of pTREPM1 plasmid. A) Lane 1, 1kb DNA ladder; lane 2, uncut plasmid; lane 3, digestion of pTREPM1 with PstI generated 1.5 and 7.7 kb fragements. B) Lane 1, uncut plasmid; lane 2, digestion of pTREPM1 with HindIII generated 3.3 and 5.8 kb fragments; lane 3, 1kb DNA ladder.

COS-7 cells failed to thrive in culture, never reaching confluence. HeLa Tet-Off cells were our next choice, since they are known to be a hearty cell line and high levels of induction have been reported in these cells (750 ± 40 fold induction) (Clontech User Manual). pTREPM1 was transfected into the HeLa Tet-Off cells and we began the process of selecting for double-stable Tet-Off cell lines. HeLa cells transfected with the vector alone (pTRE) acted as a control. The cells were selected for in the presence of hygromycin (to select for cells containing pTREPM1 or pTRE), G418 (to select for cells containing the regulatory plasmid) and Dox (to inhibit expression of PMCA1). Subsequently, we isolated 17 hygromycin/G418 resistant clones. 48 hours after Dox removal, we harvested the cells and screened by Western blot, for clones with high induction of PMCA1. As can be seen in Fig. 15, pTREPM1 (clone #5 and clone #9) contained a marginal increase in PMCA protein compared to pTRE control clones.

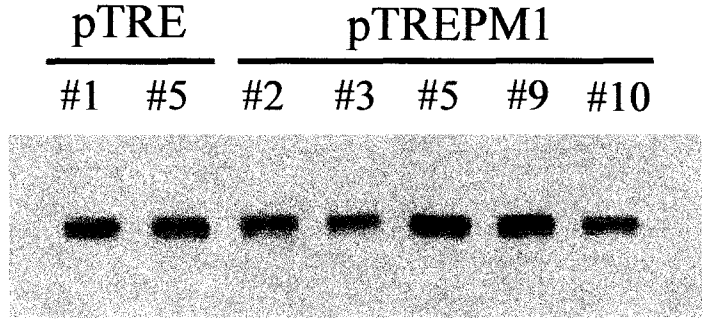

Fig. 15: Abundance of PMCA in HeLa Tet-Off pTREPM1 and pTRE stable clonal cell lines. Dox was removed to induce expression of PMCA1. 48 hrs later, crude microsomes were prepared and 15 μg of each protein sample was separated on an SDS polyacrylamide gel. Proteins were transferred to nitrocellulose and probed with anti-PMCA antibody (5F10) which recognizes a 140 kD band representing PMCA. Numbers represent different clonal cell lines.

4.0 DISCUSSION

The Results show that caloxin inhibits the PM Ca^{2+}-Mg^{2+} ATPase in erythrocyte leaky ghosts in a manner that is non-competitive with respect to the substrates ATP and Ca^{2+} and the activator calmodulin. Furthermore, caloxin inhibits formation of the phosphoenzyme intermediate starting from ^{32}P-γ-ATP, but not from ^{32}P-orthrophosphate. The first part of the Discussion will focus on the relationship of these results to literature on the reaction mechanism of the PMCA pump. Using this information, a model for inhibition of the pump by caloxin will be proposed. The Results also demonstrate that caloxin is not isoform selective. Caloxin inhibited PMCA2 and PMCA4 with low affinity, even though it was selected as an anti-PED2 of PMCA1. Experimental difficulties in overexpressing functional PMCA1 prevented us from testing our hypothesis that PMCA1 has the highest affinity for caloxin. Problems related to overexpressing the pump to high levels will be discussed.

4.1 Mechanism of action of Caloxin

An important part of our present knowledge of the catalytic and transport cycle of PMCA has been obtained using inhibitors (13, 55, 78). These inhibitors are not specific for the PMCA since they inhibit other cation transport ATPases, including SERCA and the Na^+-K^+ ATPase (11, 55). Most of these inhibitors act as substrate analogues that are able to replace the natural substrates of the pump and stabilize reaction intermediates (13, 60, 81). For example, non-hydrolyzable ATP analogues such as AMP-PCP and TNP-ADP have been used to characterize substrate binding, and the putative inorganic

phosphate (Pi) analogue, vanadate, has served a similar purpose (6, 11, 78). Fluoride complexes of aluminum and beryllium are other potential Pi analogues (35, 81). Caloxin is different from these inhibitors since 1) it is a peptide and does not structurally resemble any of the substrates of the pump, 2) it is selected for binding to an extracellular domain of the PMCA pump whereas most non-specific inhibitors bind intracellularly and 3) it is selective for the PMCA pump and does not inhibit SERCA or the Na^+-K^+ ATPase (16). The properties of caloxin, combined with the results of our study, suggest that caloxin inhibits the PMCA pump by a different mechanism than those reported for non-specific inhibitors of P-type ATPases. The relationship between our results and literature on the mechanism of action of some non-specific inhibitors of the pump will be discussed. Using information on the catalytic and transport cycle of P-type ATPases, a general model for inhibition of PMCA by caloxin will be proposed.

4.1.1 Action of Caloxin vs. non-specific inhibitors of PMCA

The effects of caloxin and non-specific inhibitors of the PMCA can be interpreted in terms of the E1-E2 model for the catalytic and transport cycle of P-type ATPases (13, 49). This model, based on functional studies of SERCA and the Na^+-K^+ ATPase, comprises a minimal number of partial reactions as outlined in Fig. 1, where E1 and E2 represent the two major conformational states of the enzyme (3, 49, 57). The sensitivity of the conformers to Ca^{2+}, ATP, ADP, Pi, and Mg^{2+} is different, making these partial reactions experimentally accessible. For example, the affinity of the E1 conformation for Ca^{2+} is high and phosphorylation by ATP is Ca^{2+}-dependent (17, 57). On the other hand, the E2 conformation has low affinity for Ca^{2+} and its phosphorylation from Pi is inhibited

by Ca^{2+} (17, 57). Inhibition of the PMCA of erythrocyte ghosts by caloxin is associated with a decrease in the level of the Ca^{2+} -dependent phosphoenzyme starting from ATP (Fig. 6A). This contrasts with the lack of effect of caloxin on formation of the Ca^{2+} -inhibited phosphoenzyme starting from Pi (Fig. 6B). Our results also show that caloxin does not compete for binding with the substrates of the pump (Figs 3-5). The observed non-competitive inhibition of PMCA by caloxin was anticipated since high affinity Ca^{2+} -binding and sites for binding to ATP and calmodulin are all on intracellular domains, whereas caloxin presumably binds extracellularly (13, 16). It is interesting to point out that inhibition of Ca^{2+} -pumps by fluorides is also non-competitive with respect to the substrates (35, 55). However, fluorides compete for phosphate, which may be considered a substrate for the reverse reaction, as it binds to the E2 conformation of the ATPase and inhibits formation of acylphosphates starting from Pi (35, 55). Caloxin did not affect the acylphosphate formation from Pi, suggesting that inhibition by caloxin does not follow the same mechanism as fluorides.

Inhibition by lanthanum (La^{3+}) also seems to occur by a different mechanism than caloxin. Lanthanum, at low concentrations (0.05 mM), increases the steady-state level of the phosphoenzyme of PMCA starting from ATP (13). Luterbacher & Schatzmann (1983) found that the phosphoenzyme accumulated in the presence of La^{3+} was the ADP-sensitive E1P form, suggesting that La^{3+} interrupts the E1P to E2P conformational transition during the catalytic cycle (37). The results of Herscher & Rega (1996) agree with this idea and suggest that La^{3+} displaces Mg^{2+} from the site from which Mg^{2+} accelerates the transition between conformers (37). However unlike La^{3+}, caloxin

decreased formation of the phophoenzyme starting from ATP, suggesting caloxin inhibition occurs by a different mechanism.

Using site-directed mutagenesis, 6 residues within putative transmembrane (TM) domains 4, 5, 6 and 8 of SERCA have been identified as integral components of the high affinity Ca^{2+} binding site(s) (17). A comparison of the primary sequences of the P-type pumps has revealed that 4 of the 6 amino acids involved in Ca^{2+} binding in the SERCA pump are conserved in the PMCA pump. Mutagenesis of these residues located in TM domain 4, 6 and 8 of PMCA, caused loss of calcium transport and the ability of the pump to form the phosphorylated intermediate starting from ATP (33). However, phosphorylation of Glu423Ala (in TM domain 4) and Asp883Asn (in TM domain 6) mutant enzymes with Pi was observed even in the presence of calcium, which inhibits phosphorylation in the wild-type enzyme possessing intact high affinity calcium-binding sites. This suggests that the phenotype of the PMCA mutants is consistent with disruption of the high-affinity binding of calcium, which is supported by the observed stabilization of the E2 intermediate (the intermediate formed from Pi), even in the presence of calcium (33). Caloxin also appears to stabilize the E2 conformation, since it allows phosphoenzyme formation from Pi but inhibits phosphoenzyme formation from ATP, however we did not test the effect of caloxin on the Ca^{2+} sensitive formation of the phosphoenzyme from Pi. Using this knowledge, a general model for inhibition of PMCA by caloxin will be presented.

4.1.2 Model for Caloxin inhibition

Caloxin was selected for binding to the second extracellular domain (PED2) of PMCA1, but it produced complete inhibition of PMCA in erythrocyte ghosts, which express mainly PMCA4 (16). It is not clear how binding to an extracellular site leads to inhibition of the pump. A mechanism linked to altered protein conformation may explain the inhibitory effect of caloxin. Its binding may produce an inhibitory perturbation that is transmitted from the extracellular binding site to the transmembrane and/or intracellular domains of the pump. These conformational changes may affect substrate (Ca^{2+}, ATP, calmodulin) binding, phosphate binding or its hydrolysis, thereby disrupting one or more of the partial reactions comprising the catalytic and transport cycle of the pump (Fig. 1). Caloxin inhibited formation of the phosphoenzyme intermediate starting from ATP, but not from Pi, suggesting that caloxin may favor the E2 conformation of the pump. The decrease in the level of phosphoenzyme does not necessarily imply that caloxin blocks the phosphorylation reaction itself. The amount of phosphoenzyme will also decrease if caloxin inhibits other partial reactions of the pump, such as Ca^{2+} or ATP binding or the E2-to-E1 conversion (6, 17, 35). However, it is interesting that a conserved residue in TM domain 4 of PMCA is implicated in high affinity calcium-binding, with mutagenesis of this residue having similar effects as caloxin on acylphosphate formation from ATP and Pi (33) (see 4.1.1 for details). Caloxin binds to PED2 of PMCA, which connects TM domains 3 and 4, suggesting that caloxin binding may induce conformational changes that disrupt calcium binding and/or translocation associated with TM domain 4. Future experiments testing the effect of caloxin on calcium sensitive reactions (like phosphorylation from Pi) must be performed to test this hypothesis.

4.2 Overexpression of PMCA

To understand the effects of caloxin on the different isoforms of PMCA, one must obtain overexpression systems, as each tissue expresses more than one isoform of the pump. Furthermore, it is important to use cell lines that have low-level PMCA expression, yet permit overexpression at very high levels. A mammalian expression system (COS-1) has been extensively used to study the properties of the SERCA pump (17, 36). However, overexpression of the PMCA pump in this system – as well as in others - has been more difficult. When successful, the amount of active PMCA protein expressed, as compared to that of the SERCA pump, has been substantially smaller (36). Generally, only 3 to 6 times the basal level of PMCA activity is observed in COS cells transiently transfected with PMCA (1, 36). The reasons for the modest levels of active PCMA pump overexpression compared to SERCA may be linked to the central role that PMCA plays in cell function, since it is thought to be constitutively active in order to maintain the low resting levels of cytosolic Ca^{2+} (13, 28, 29). On the other hand, SERCA may be primarily active following a cell-signaling event (28, 29). Therefore, the expression of PMCA at high levels may be toxic to the cell, as this would mean that cells would be unable to maintain cytosolic Ca^{2+} at levels necessary for cell function, like cell proliferation. In fact, Husain et al (1997) reported that transient overexpression of PMCA1a in vascular smooth muscle cells (VSMC) elevates the ^{45}Ca efflux rate 2-fold and reduces the rate of cell proliferation 2.5-fold, suggesting a critical role for PMCA in the regulation of VSMC growth (40). However, Guerini et al (1995) and Liu et al (1996) showed that overexpression of PMCA4 and PMCA1 respectively in stable cell clones,

had little effect on cell growth, although in both cases, numerous compensatory changes in calcium homeostatic mechanisms (eg SERCA) were reported, suggesting physiological adaptations in these PMCA cell clones (32, 50). The relatively low and similar activity of PMCA from different sources (tissues and species) may well be related to the existence of an optimal activity of this enzyme. Still, unknown intracellular regulatory mechanisms may exist to prevent the overproduction of the pump protein in cells. Another reason for the lower expression levels of PMCA compared to SERCA may be the particular susceptibility of PMCA to intracellular proteases. It has been shown that the PMCA pump is sensitive to the action of the intracellular Ca^{2+}-dependent protease calpain as compared to the SERCA pump, which is completely resistant to it (36). It is perhaps for these reasons that there are only a limited number of studies on cells overexpressing PMCA even though there are a larger number of studies on the overexpression of SERCA.

Among the pump isoforms, PMCA4 has been studied most extensively, and its overexpression is well documented (1, 32, 36, 65, 67). Discrepancies exist however, between the amount of PMCA4 protein formed and its overall function in the cells (1). PMCA4 was successfully expressed in our study and used for caloxin inhibition. The values for PMCA4 protein expression level and PMCA4 activity are similar to those reported previously for overexpression of PMCA4 in the COS cell system (1, 36). Other isoforms of the pump have been overexpressed in mammalian cells only recently, and with limited success. Expression of PMCA2 in insect cells using a baculovirus system has been more favorable (67). A limited amount of microsomes isolated from these cells were obtained from another lab, and we were able to show caloxin inhibition of PMCA2.

In this study we also had limited success with expressing PMCA3 in COS-M6 cells. However, since caloxin had been obtained as a peptide that would bind to PED2 of PMCA1, it was more important to obtain a cell system overexpressing this isoform.

There are only 2 reports on the successful overexpression of PMCA1. Husain et al (1997) reported 2- to 4-fold increased levels of PMCA1a mRNA and protein following transient transfection into vascular smooth muscle cells (VSMC) (40). Liu et al (1996) showed overexpression of PMCA1a in endothelial cell clones to modest levels (50). We approached these groups for the PMCA1 plasmids, however they were not made available to us (personal communication), requiring us to make our own PMCA1 plasmid. Furthermore, these groups have not published any work using PMCA1 overexpressing cells since 1997. In transient transfections of pcDNAPM1 into COS-M6 cells, we detected a modest increase in the expression level of PMCA1 protein (using Western blot analysis), however this increase was not associated with an increase in the Ca^{2+}-Mg^{2+} ATPase activity. The possibility exists that the protein may have been incorrectly processed and/or targeted, interfering with its ability to adopt the proper conformation necessary for functional ATPase activity (1). Another possibility for the discrepancy is that the level of expression of PMCA1 was too low to be detected functionally by the coupled enzyme assay. We also attempted overexpression of PMCA1 in an inducible system, but we were unsuccessful in obtaining cells that expressed high levels of PMCA1. Finally, we cannot rule out the existence of errors in the original PMCA1 cDNA cloned from the rat brain cDNA library that was used to make our PMCA1 constructs.

4.2.1 Comparison of Effects of Caloxin on PMCA Isoforms

The putative second extracellular domain (PED2) sequences of human PMCAs 1 to 4 are mostly identical except for two major differences: glutamine at amino acid position 400 in PMCA1 vs. glutamic acid in PMCA3, and alanine at position 406 in PMCA1 vs. proline in PMCA2 and 4 (Fig. 2). Caloxin was selected as an anti-PED2 of PMCA1. Even though erythrocytes express mainly PMCA4 (and some PMCA1), caloxin inhibits erythrocyte Ca^{2+}-Mg^{2+} ATPase activity with an inhibition constant of 0.4 ± 0.1 mM (16). This suggests that caloxin is not isoform selective. However, it does not exclude the possibility that PMCA1 has the highest affinity for caloxin. Unfortunately we were unable to test the effect of caloxin on PMCA1 activity, though caloxin inhibited PMCA4 and PMCA2 (producing similar inhibition at 1.87 mM), supporting the hypothesis that caloxin is not isoform selective.

We anticipated that PMCA4 would have a similar affinity for caloxin as reported for erythrocytes, since they contain mainly PMCA4. Caloxin has a Ki of 1.3 ± 0.1 mM for PMCA4. Since erythrocytes also contain some PMCA1, the higher affinity of the erythrocyte PMCA for caloxin (0.4 ± 0.1 mM) could be due to the presence of PMCA1 in these membranes, assuming that PMCA1 has a relatively high affinity for caloxin since it was used to screen for caloxin.

4.3 Conclusion

Currently there are no known functions of the extracellular domains of PMCA. They are considered to be no more than peptide segments that connect the TM domains. Caloxin inhibits the PMCA pump in a manner which is non-competitive with respect to

the substrates Ca^{2+} and ATP and the activator calmodulin. Furthermore, caloxin inhibits the acylphosphate formation from ATP, but not from inorganic phosphate. These results suggest that it is possible to affect the activity of PMCA by perturbing one of its extracellular domains. Hopefully, this recognition will pave the way for the discovery of a new class of extracellular modulators of PMCA.

5.0 REFERENCES

1. Adamo HP, Verma AK, Sanders MA, et al. Overexpression of the erythrocyte plasma membrane Ca2+ pump in COS-1 cells. Biochem J 1992;285 (Pt 3):791-7.

2. Alberts B. Molecular Biology of the Cell. Third Edition ed. New York & London: Garland Publishing Inc.; 1994.

3. Andersen JP, Vilsen B. Structure-function relationships of cation translocation by Ca(2+)- and Na+, K(+)-ATPases studied by site-directed mutagenesis. FEBS Lett 1995;359:101-6.

4. Arystarkhova E, Gasparian M, Modyanov NN, Sweadner KJ. Na,K-ATPase extracellular surface probed with a monoclonal antibody that enhances ouabain binding. J Biol Chem 1992;267:13694-701.

5. Ausubel FM. Current Protocols in Molecular Biology. Toronto: Greene Publishing Associates & Wiley Interscience; 1988.

6. Barrabin H, Garrahan PJ, Rega AF. Vanadate inhibition of the Ca2+-ATPase from human red cell membranes. Biochim Biophys Acta 1980;600:796-804.

7. Barritt GJ. Receptor-activated Ca2+ inflow in animal cells: a variety of pathways tailored to meet different intracellular Ca2+ signalling requirements. Biochem J 1999;337 (Pt 2):153-69.

8. Berridge MJ. The molecular basis of communication within the cell. Sci Am 1985;253:142-52.

9. Blaustein MP, Lederer WJ. Sodium/calcium exchange: its physiological implications. Physiol Rev 1999;79:763-854.

10. Brandt P, Neve RL, Kammesheidt A, Rhoads RE, Vanaman TC. Analysis of the tissue-specific distribution of mRNAs encoding the plasma membrane calcium-pumping ATPases and characterization of an alternately spliced form of PMCA4 at the cDNA and genomic levels. J Biol Chem 1992;267:4376-85.

11. Cantley LC, Jr., Resh MD, Guidotti G. Vanadate inhibits the red cell (Na+, K+) ATPase from the cytoplasmic side. Nature 1978;272:552-4.

12. Carafoli E. The signaling function of calcium and its regulation. Journal of Hypertension 1994;12:S47-S56.

13. Carafoli E. Calcium pump of the plasma membrane. Physiol Rev 1991;71:129-53.

14. Carafoli E. The Ca2+ pump of the plasma membrane. J Biol Chem 1992;267:2115-8.

15. Carafoli E. Biogenesis: plasma membrane calcium ATPase: 15 years of work on the purified enzyme. FASEB J 1994;8:993-1002.

16. Chaudhary J, Walia M, Matharu J, Escher E, Grover AK. Caloxin: a novel plasma membrane Ca2+ pump inhibitor. Am J Physiol Cell Physiol 2001;280:C1027-C1030.

17. Clarke DM, Loo TW, Inesi G, MacLennan DH. Location of high affinity Ca2+-binding sites within the predicted transmembrane domain of the sarcoplasmic reticulum Ca2+-ATPase. Nature 1989;339:476-8.

18. Dumont RA, Lins U, Filoteo AG, et al. Plasma membrane Ca2+-ATPase isoform 2a is the PMCA of hair bundles. J Neurosci 2001;21:5066-78.

19. Enyedi A, Elwess NL, Filoteo AG, et al. Protein kinase C phosphorylates the "a" forms of plasma membrane Ca2+ pump isoforms 2 and 3 and prevents binding of calmodulin. J Biol Chem 1997;272:27525-8.

20. Falchetto R, Vorherr T, Brunner J, Carafoli E. The plasma membrane Ca2+ pump contains a site that interacts with its calmodulin-binding domain. J Biol Chem 1991;266:2930-6.

21. Fasolato C, Innocenti B, Pozzan T. Receptor-activated Ca2+ influx: how many mechanisms for how many channels? Trends Pharmacol Sci 1994;15:77-83.

22. Feschenko MS, Zvaritch EI, Hofmann F, et al. A monoclonal antibody recognizes an epitope in the first extracellular loop of the plasma membrane Ca2+ pump. J Biol Chem 1992;267:4097-101.

23. Filoteo AG, Gorski JP, Penniston JT. The ATP-binding site of the erythrocyte membrane Ca2+ pump. Amino acid sequence of the fluorescein isothiocyanate-reactive region. J Biol Chem 1987;262:6526-30.

24. Filoteo AG, Elwess NL, Enyedi A, et al. Plasma membrane Ca2+ pump in rat brain. Patterns of alternative splices seen by isoform-specific antibodies. J Biol Chem 1997;272:23741-7.

25. Garcia ML, Strehler EE. Plasma membrane calcium ATPases as critical regulators of calcium homeostasis during neuronal cell function. Front Biosci 1999;4:D869-D882.

26. Ghosh TK, Bian JH, Short AD, Rybak SL, Gill DL. Persistent intracellular calcium pool depletion by thapsigargin and its influence on cell growth. J Biol Chem 1991;266:24690-7.

27. Greeb J, Shull GE. Molecular cloning of a third isoform of the calmodulin-sensitive plasma membrane Ca2+-transporting ATPase that is expressed predominantly in brain and skeletal muscle. J Biol Chem 1989;264:18569-76.

28. Grover AK. Ca-pumps in smooth muscle: one in plasma membrane and another in endoplasmic reticulum. Cell Calcium 1985;6:227-36.

29. Grover AK, Samson SE. Pig coronary artery smooth muscle: substrate and pH dependence of the two calcium pumps. Am J Physiol 1986;251:C529-C534.

30. Grover AK, Khan I. Calcium pump isoforms: diversity, selectivity and plasticity. Review article. Cell Calcium 1992;13:9-17.

31. Grover AK, Xu A, Samson SE, Narayanan N. Sarcoplasmic reticulum Ca2+ pump in pig coronary artery smooth muscle is regulated by a novel pathway. Am J Physiol 1996;271:C181-C187.

32. Guerini D, Schroder S, Foletti D, Carafoli E. Isolation and characterization of a stable Chinese hamster ovary cell line overexpressing the plasma membrane Ca(2+)-ATPase. J Biol Chem 1995;270:14643-50.

33. Guerini D, Foletti D, Vellani F, Carafoli E. Mutation of conserved residues in transmembrane domains 4,6 and 8 causes loss of Ca2+ transport by the plasma membrane Ca2+ pump. Biochemistry 1996;35:3290-6.

34. Hao L, Rigaud JL, Inesi G. Ca2+/H+ countertransport and electrogenicity in proteoliposomes containing erythrocyte plasma membrane Ca-ATPase and exogenous lipids. J Biol Chem 1994;269:14268-75.

35. Hawkins C, Xu A, Narayanan N. Comparison of the effects of fluoride on the calcium pumps of cardiac and fast skeletal muscle sarcoplasmic reticulum: evidence for tissue- specific qualitative difference in calcium-induced pump conformation. Biochim Biophys Acta 1994;1191:231-43.

36. Heim R, Iwata T, Zvaritch E, et al. Expression, purification, and properties of the plasma membrane Ca2+ pump and of its N-terminally truncated 105-kDa fragment. J Biol Chem 1992;267:24476-84.

37. Herscher CJ, Rega AF. Pre-steady-state kinetic study of the mechanism of inhibition of the plasma membrane Ca(2+)-ATPase by lanthanum. Biochemistry 1996;35:14917-22.

38. Hilfiker H, Strehler-Page MA, Stauffer TP, Carafoli E, Strehler EE. Structure of the gene encoding the human plasma membrane calcium pump isoform 1. J Biol Chem 1993;268:19717-25.

39. Holda JR, Klishin A, Sedova M, Huser J, Blatter LA. Capacitative Calcium Entry. News Physiol Sci 1998;13:157-63.

40. Husain M, Jiang L, See V, et al. Regulation of vascular smooth muscle cell proliferation by plasma membrane Ca(2+)-ATPase. Am J Physiol 1997;272:C1947-C1959.

41. James P, Maeda M, Fischer R, et al. Identification and primary structure of a calmodulin binding domain of the Ca2+ pump of human erythrocytes. J Biol Chem 1988;263:2905-10.

42. Jarrett HW, Penniston JT. Purification of the Ca2+-stimulated ATPase activator from human erythrocytes. Its membership in the class of Ca2+-binding modulator proteins. J Biol Chem 1978;253:4676-82.

43. Jarrett HW, Kyte J. Human erythrocyte calmodulin. Further chemical characterization and the site of its interaction with the membrane. J Biol Chem 1979;254:8237-44.

44. Jeffery DA, Roufogalis BD, Katz S. The effect of calmodulin on the phosphoprotein intermediate of Mg2+- dependent Ca2+-stimulated adenosine triphosphatase in human erythrocyte membranes. Biochem J 1981;194:481-6.

45. Keeton TP, Burk SE, Shull GE. Alternative splicing of exons encoding the calmodulin-binding domains and C termini of plasma membrane Ca(2+)-ATPase isoforms 1, 2, 3, and 4. J Biol Chem 1993;268:2740-8.

46. Khan I, Grover AK. Expression of cyclic-nucleotide-sensitive and -insensitive isoforms of the plasma membrane Ca2+ pump in smooth muscle and other tissues. Biochem J 1991;277 (Pt 2):345-9.

47. Kozel PJ, Friedman RA, Erway LC, et al. Balance and hearing deficits in mice with a null mutation in the gene encoding plasma membrane Ca2+-ATPase isoform 2. J Biol Chem 1998;273:18693-6.

48. Laemmli UK. Cleavage of structural proteins during the assembly of the head of bacteriophage T4. Nature 1970;227:680-5.

49. Lee AG, East JM. What the structure of a calcium pump tells us about its mechanism. Biochem J 2001;356:665-83.

50. Liu BF, Xu X, Fridman R, Muallem S, Kuo TH. Consequences of functional expression of the plasma membrane Ca2+ pump isoform 1a. J Biol Chem 1996;271:5536-44.

51. Luterbacher S, Schatzmann HJ. The site of action of La3+ in the reaction cycle of the human red cell membrane Ca2+-pump ATPase. Experientia 1983;39:311-2.

52. Marin J, Encabo A, Briones A, Garcia-Cohen EC, Alonso MJ. Mechanisms involved in the cellular calcium homeostasis in vascular smooth muscle: calcium pumps. Life Sci 1999;64:279-303.

53. Merritt JE, McCarthy SA, Davies MP, Moores KE. Use of fluo-3 to measure cytosolic Ca2+ in platelets and neutrophils. Loading cells with the dye, calibration of traces, measurements in the presence of plasma, and buffering of cytosolic Ca2+. Biochem J 1990;269:513-9.

54. Mintz E, Guillain F. Ca2+ transport by the sarcoplasmic reticulum ATPase. Biochim Biophys Acta 1997;1318:52-70.

55. Missiaen L, Wuytack F, De Smedt H, Vrolix M, Casteels R. AlF4- reversibly inhibits 'P'-type cation-transport ATPases, possibly by interacting with the phosphate-binding site of the ATPase. Biochem J 1988;253:827-33.

56. Missiaen L, Wuytack F, Raeymaekers L, et al. Ca2+ extrusion across plasma membrane and Ca2+ uptake by intracellular stores. Pharmacol Ther 1991;50:191-232.

57. Moller JV, Juul B, le Maire M. Structural organization, ion transport, and energy transduction of P- type ATPases. Biochim Biophys Acta 1996;1286:1-51.

58. Muallem S, Karlish SJ. Regulatory interaction between calmodulin and ATP on the red cell Ca2+ pump. Biochim Biophys Acta 1980;597:631-6.

59. Muallem S, Beeker T, Pandol SJ. Role of Na+/Ca2+ exchange and the plasma membrane Ca2+ pump in hormone- mediated Ca2+ efflux from pancreatic acini. J Membr Biol 1988;102:153-62.

60. Murphy AJ, Coll RJ. Fluoride is a slow, tight-binding inhibitor of the calcium ATPase of sarcoplasmic reticulum. J Biol Chem 1992;267:5229-35.

61. Niggli V, Adunyah ES, Penniston JT, Carafoli E. Purified (Ca2+-Mg2+)-ATPase of the erythrocyte membrane. Reconstitution and effect of calmodulin and phospholipids. J Biol Chem 1981;256:395-401.

62. Niggli V, Adunyah ES, Carafoli E. Acidic phospholipids, unsaturated fatty acids, and limited proteolysis mimic the effect of calmodulin on the purified erythrocyte Ca2+ - ATPase. J Biol Chem 1981;256:8588-92.

63. Niggli V, Sigel E, Carafoli E. The purified Ca2+ pump of human erythrocyte membranes catalyzes an electroneutral Ca2+-H+ exchange in reconstituted liposomal systems. J Biol Chem 1982;257:2350-6.

64. Paschen W. Dependence of vital cell function on endoplasmic reticulum calcium levels: implications for the mechanisms underlying neuronal cell injury in different pathological states. Cell Calcium 2001;29:1-11.

65. Paszty K, Verma AK, Padanyi R, et al. Plasma membrane Ca2+ATPase isoform 4b is cleaved and activated by caspase-3 during the early phase of apoptosis. J Biol Chem 2002;277:6822-9.

66. Penheiter AR, Filoteo AG, Croy CL, Penniston JT. Characterization of the deafwaddler mutant of the rat plasma membrane calcium-ATPase 2. Hear Res 2001;162:19-28.

67. Penheiter AR, Caride AJ, Enyedi A, Penniston JT. Tryptophan 1093 is largely responsible for the slow off rate of calmodulin from plasma membrane Ca2+ pump 4b. J Biol Chem 2002;277:17728-32.

68. Richards DE, Rega AF, Garrahan PJ. Two classes of site for ATP in the Ca2+-ATPase from human red cell membranes. Biochim Biophys Acta 1978;511:194-201.

69. Rose AM, Valdes R, Jr. Understanding the sodium pump and its relevance to disease. Clin Chem 1994;40:1674-85.

70. Schatzmann HJ. ATP-dependent Ca++-extrusion from human red cells. Experientia 1966;22:364-5.

71. Schulze D, Kofuji P, Hadley R, et al. Sodium/calcium exchanger in heart muscle: molecular biology, cellular function, and its special role in excitation-contraction coupling. Cardiovasc Res 1993;27:1726-34.

72. Shull GE, Greeb J. Molecular cloning of two isoforms of the plasma membrane Ca2+- transporting ATPase from rat brain. Structural and functional domains exhibit similarity to Na+,K+- and other cation transport ATPases. J Biol Chem 1988;263:8646-57.

73. Shull GE. Gene knockout studies of Ca2+-transporting ATPases. Eur J Biochem 2000;267:5284-90.

74. Stauffer TP, Guerini D, Carafoli E. Tissue distribution of the four gene products of the plasma membrane Ca2+ pump. A study using specific antibodies. J Biol Chem 1995;270:12184-90.

75. Strehler EE, James P, Fischer R, et al. Peptide sequence analysis and molecular cloning reveal two calcium pump isoforms in the human erythrocyte membrane. J Biol Chem 1990;265:2835-42.

76. Strehler EE, Zacharias DA. Role of alternative splicing in generating isoform diversity among plasma membrane calcium pumps. Physiol Rev 2001;81:21-50.

77. Taylor CW, Traynor D. Calcium and inositol trisphosphate receptors. J Membr Biol 1995;145:109-18.

78. Tiffert T, Lew VL. Kinetics of inhibition of the plasma membrane calcium pump by vanadate in intact human red cells. Cell Calcium 2001;30:337-42.

79. Towbin H, Staehelin T, Gordon J. Electrophoretic transfer of proteins from polyacrylamide gels to nitrocellulose sheets: procedure and some applications. Proc Natl Acad Sci U S A 1979;76:4350-4.

80. Treiman M, Caspersen C, Christensen SB. A tool coming of age: thapsigargin as an inhibitor of sarco-endoplasmic reticulum Ca(2+)-ATPases. Trends Pharmacol Sci 1998;19:131-5.

81. Troullier A, Girardet JL, Dupont Y. Fluoroaluminate complexes are bifunctional analogues of phosphate in sarcoplasmic reticulum Ca(2+)-ATPase. J Biol Chem 1992;267:22821-9.

82. Verma AK, Filoteo AG, Stanford DR, et al. Complete primary structure of a human plasma membrane Ca2+ pump. J Biol Chem 1988;263:14152-9.

83.Zvaritch E, James P, Vorherr T, et al. Mapping of functional domains in the plasma membrane Ca2+ pump using trypsin proteolysis. Biochemistry 1990;29:8070-6.

84. Darby PJ, Kwan CY, Daniel EE. Caveolae from canine airway smooth muscle contain the necessary components for a role in Ca(2+) handling. Am J Physiol Lung Cell Mol Physiol 2000:279(6):L1226-35.